The NEDD8 inhibitor MLN4924 increases the size of the nucleolus and activates p53 through the ribosomal-Mdm2 pathway

Bailly, A.; Perrin, A.; Bou Malhab, L. J.; Pion, E.; Larance, M.; Nagala, M.; Smith, P.; O'Donohue, M.-F.; Gleizes, P.-E.; Zomerdijk, Josephus; Lamond, A. I.; Xirodimas, D. P.

Published in:
Oncogene

DOI:
10.1038/onc.2015.104

Publication date:
2016

Document Version
Peer reviewed version

The NEDD8 inhibitor MLN4924 increases the size of the nucleolus and activates p53 through the ribosomal-Mdm2 pathway

Aymeric Bailly[1], Aurelien Perrin[1#], Lara Bou Malhab[1#], Emmanuelle Pion[1], Mark Larance[2], Manjula Nagala[2], Peter Smith[3], Marie-Françoise O'Donohue[4], Pierre-Emmanuel Gleizes[4], Joost Zomerdijk[2], Angus I. Lamond[2] and Dimitris P. Xirodimas[1*]

[1]Centre de Recherche de Biochimie Macromoléculaire - UMR 5237, CNRS, Route de Mende 34 293, Montpellier, Cedex 5, France

[2]Centre for Gene Regulation and Expression, College of Life Sciences, University of Dundee, Dow Street, Dundee, DD1 5EH, Scotland/UK

[3]Millennium Pharmaceuticals Inc., 40 Landsdowne Street, Cambridge, MA 02139, USA

[4]Laboratoire de Biologie Moléculaire Eucaryote, UMR CNRS 5099, Bâtiment IBCG, 118 route de Narbonne, 31062 Toulouse Cedex 9, France

# These authors contributed equally to this work

*corresponding author

tel: +44 1382 386303

fax: +44 1382 386375

email: dimitris.xirodimas@crbm.cnrs.fr

Running title: MLN4924 targets the nucleolus

'The NEDD8 inhibitor MLN4924 increases the size of the nucleolus and activates p53 through the ribosomal-Mdm2 pathway', Oncogene 35:4 (2015), http://dx.doi.org/10.1038/onc.2015.104

Abstract

The ubiquitin like molecule NEDD8 is essential for viability, growth and development and is a potential target for therapeutic intervention. We found that the small molecule inhibitor of NEDDylation MLN4924 alters the morphology and increases the surface size of the nucleolus in human and in germline cells of *C. elegans* in the absence of nucleolar fragmentation. SILAC proteomics and monitoring of rRNA production, processing and ribosome profiling shows that MLN4924 changes the composition of the nucleolar proteome but does not inhibit RNA Pol I transcription. Further analysis demonstrates that MLN4924 activates the p53 tumour suppressor through the RPL11/RPL5-Mdm2 pathway, with characteristics of nucleolar stress. The study identifies the nucleolus as a target of inhibitors of NEDDylation and provides a mechanism for p53 activation upon NEDD8 inhibition. It also indicates that targeting the nucleolar proteome without affecting nucleolar transcription initiates the required signalling events for the control of cell cycle regulators.

Keywords: NEDD8, MLN4924, nucleolus, ribosomal proteins, p53, Mdm2

Introduction

The NEDD8 ubiquitin like molecule is vital for a range of processes including cell viability, growth and development. Covalent modification of NEDD8 is initiated by the processing of the C-terminal tail to expose a di-glycine motif. This mature/processed form of NEDD8 is activated by an E1 activating enzyme (known as APPBP1/Uba3 or NAE) and is transferred to substrate proteins through the action of E2 conjugating enzymes and E3-ligase [1, 2, 3, 4]. Several targets for NEDD8 have been identified but the most well-characterised substrate is the cullin family of proteins [5, 6]. Cullins are scaffold components for RING E3-ubiquitin ligases, called CRL (Cullin Ring Ligases). NEDDylation of cullins stimulates the activity of the E3-ligase, resulting in increased degradation of substrate proteins through the Ubiquitin Proteasome System (UPS) [7, 8]. It is estimated that CRLs have several hundred substrates, including cell cycle regulators, components of the DNA replication machinery and mediators of cellular stress, such as hypoxia and oxidative stress [7, 9]. Therefore, a well-described function of NEDD8 is to promote protein degradation through UPS. This knowledge combined with the fact that the inhibitor of the proteasome, bortezomib (Velcade®), is used for the treatment of various types of myeloma and lymphoma, prompted development of specific inhibitors of the NEDD8 machinery [4, 10]. MLN4924 is a small molecule that specifically inhibits the NEDD8 pathway [11, 12]. Treatment of tumour cells with MLN4924 can induce apoptosis, and in vivo MLN4924 shows anti-tumour activity in mice harbouring human xenografts for solid and hematologic tumours [11]. These encouraging preclinical studies with MLN4924 provided the rationale for early phase clinical studies [1, 4]. Therefore, elucidation of pathways controlled by NEDD8 becomes increasingly important. Recent studies showed that inhibition of NEDDylation by MLN4924 activates the p53

tumour suppressor and that the p53 pathway is relevant for the biological response to MLN4924 treatment [13, 14]. Interestingly, MLN4924-induced apoptosis is increased upon knockdown of p53 in tumour cell lines containing wild type p53, suggesting that p53 activation may protect cells against MLN4924 [13]. However, the mechanism for the MLN4924-induced p53 activation remains elusive.

The nucleolus is the subnuclear structure at the centre of ribosomal RNA (rRNA) transcription and ribosome subunit production, and is thus essential for protein synthesis and cell growth [15, 16, 17]. What is also evident is that the nucleolus is not a static subnuclear structure but responds to a great variety of cellular stresses. DNA damage induced by ionizing radiation, UV or chemotherapeutic drugs, inhibition of RNA Pol I transcription by nutrient starvation or Actinomycin D (ActD), proteasome inhibition and viral infection, can all change nucleolar structure and alter the nucleolar proteome [18, 19, 20, 21, 22, 23].

Induction of nucleolar stress elicits signalling events with important biological consequences for cell cycle progression. For example, the p53 tumour suppressor responds to the majority of known nucleolar stressors, with the best characterized being the inhibition of RNA Pol I transcription [24]. Low doses of ActD specifically inhibit RNA Pol I and thus the production of rRNA in the nucleolus [25]. Under these conditions, several RPs have been reported to block Mdm2 E3-ligase activity towards p53 through direct binding to Mdm2. In particular, for RPL11 and RPL5, a co-operation between the 2 RPs and 5S rRNA enhances Mdm2 inhibition under ribosomal stress conditions [26, 27]. This causes p53 stabilisation, activation of the p53 response and cell cycle arrest [28, 29, 30 ,31].

We found that inhibition of NEDDylation by MLN4924 alters the morphology and increases the surface size of the nucleolus in the absence of nucleolar fragmentation

both in human cells and in *C. elegans* germline cells. Combination of SILAC quantitative proteomics, rRNA production/processing and ribosome profiling show that in contrast to the established nucleolar stressor ActD, MLN4924 alters the nucleolar proteome but does not affect RNA Pol I transcription. Further analysis shows that MLN4924 activates the p53 pathway through the RP-Mdm2 module with characteristics of nucleolar stress. This study reveals that MLN4924 causes activation of key tumour suppressor pathways through the nucleolus. Furthermore, the data support a conserved role for NEDDylation as a regulator of nucleolar signaling. As MLN4924 is currently being tested in clinical trials, this study identifies the nucleolus as a target for the action of a potential novel chemotherapeutic drug.

Results

MLN4924 increases the surface size of the nucleolus in human cells and in *C. elegans* germline cells

Inhibition of NEDDylation by MLN4924 produces diverse biological effects mainly through inhibition of CRL function. We observed that treatment with MLN4924 altered the morphology of the nucleolus without detectable nucleolar fragmentation (Fig. 1A). To investigate in more detail the effect of MLN4924 on nucleolar organisation, we monitored the effect of MLN4924 on the localization of nucleolar proteins that reside within distinct areas in the nucleolus. U2OS cells were either untreated or treated with MLN4924 and the localization of nucleolin and fibrillarin (dense fibrillar component) and B23/nucleophosmin (granular component) was monitored. MLN4924 has no effect on the localization of any of the tested nucleolar proteins, confirming that MLN4924 affects the morphology but not the integrity of the nucleolus (Fig. 1B). We also observed that the surface size of the nucleolus is altered in the MLN4924 treated compared to untreated cells. We designed an experiment, similar to that described by Nicholas Baker [32], to quantify changes in the nucleolar surface size under different conditions. We performed fibrillarin and DAPI staining to define the nucleolus and the nucleus area respectively using the same cross-sectional areas. To provide a measure of nucleolar and nuclear surface area, we determined the number of pixels by defining the minimal and maximal thresholds independent of labelling intensity, as described in supplementary information. The ratio of the nucleolar to nuclear area determines the relative changes in nucleolar size under different conditions. MLN4924 caused a significant increase in nucleolar surface area compared to control cells (Fig. 1C, D). As controls we used the chemotherapeutic drugs ActD and doxorubicin that cause nucleolar segregation (Fig.

1E). Protein NEDDylation is a highly conserved post-translational modification. We used *C. elegans* as a model organism to determine the conservation of our observations on the effect of NEDD8 inhibition on nucleolar morphology and to also establish the physiology of our observations at organism level. We treated *C. elegans* with MLN4924 and performed similar analysis on the surface area of the nucleolus to that performed in human cells [33]. We focused on germline cells as they rapidly proliferate and contain relatively large nucleoli that can be easily monitored and studied. Animals were either untreated or treated with MLN4924 and germline cells were dissected and stained for fibrillarin and with DAP1 to determine the nucleolar and nuclear area as before. We found that similarly to what is observed in human cells MLN4924 caused a significant increase in nucleolar surface area (Fig. 2A, B). Similar results were obtained with siRNA against the *C. elegans* NEDD8 (NED-8) (Fig. 2A, B). Application of genotoxic treatments including UV, ActD, or doxorubicin caused the formation of either distinct nucleolar fragments (UV) or sub-fragmentation (segregation) within the defined nucleolar area (ActD and doxorubicin) (Fig. 2C). The above data identify a role for NEDD8 in controlling nucleolar morphology and surface area, which is conserved between humans and *C. elegans.*

MLN4924 activates p53 through the RP-Mdm2 pathway

Changes in the nucleolar morphology usually reflect changes in the nucleolar function, which are detected by multiple cell cycle regulators [23]. The p53 tumour suppressor is a sensitive sensor of nucleolar misfunction. Ribosomal proteins are key players in transmitting defects in nucleolar function to p53 through inhibition of the Mdm2 E3-ligase [30]. We hypothesized that if p53 activation by MLN4924 is due to the observed changes in nucleolar morphology, it should depend on the RP-Mdm2 signalling pathway. Further evidence to support this hypothesis derive from previous

studies that showed that inhibition of NEDDylation of RPL11 participates in p53 activation upon nucleolar stress [34].

MCF7 cells, which contain wild type endogenous p53 were treated with increasing doses of MLN4924. As expected, MLN4924 decreased Cullin-1 NEDDylation (Fig. 3A). MLN4924 also increased p53 levels in a dose-dependent manner and the expression of p53 regulated genes [35], consistent with previous studies and with the notion that inhibition of NEDDylation causes p53 activation (Fig. 3A). Similar effects of MLN4924 were observed in other p53 positive cell lines, including U2OS, HCT116 and A375 (data not shown).

We next determined the effect of MLN4924 on L11 NEDDylation. H1299 cells were transiently transfected with plasmid vectors encoding Flag-L11 and His_6-NEDD8. His_6-NEDDylated proteins were isolated by Ni-agarose chromatography and blotted for Flag-L11. MLN4924 decreased RPL11 NEDDylation (pull-down) relative to total levels of RPL11 (whole extracts) (Fig. 3B). Consistent with the notion that prolonged inhibition of NEDDylation also leads to RPL11 degradation, MLN4924 decreased the total levels of RPL11 (Fig. 3B) [34, 36]. The nucleolus is a dynamic structure, and it has been established that nucleolar disruption correlates with altered mobility kinetics of many nucleolar proteins [36, 37, 38]. We used live cell imaging and Fluorescence Recovery After Photobleaching (FRAP) to determine the effect of MLN4924 on the mobility of RPL11. We used H1299 cells stably expressing RPL11-EGFP that were either untreated or treated with MLN4924. As control we used Actinomycin D, which is known to affect the mobility of ribosomal proteins [36, 37, 38, 39]. By measuring in real time the recovery of the EGFP signal in the nucleolus after bleaching, we found that both MLN4924 and ActD decreased the mobility of RPL11-EGFP (Fig. 3C).

The data suggest that MLN4924 may impact on p53 function through mechanisms involving RPL11. To determine the role of RPL11 in p53 stabilisation by MLN4924 we transfected MCF7 cells either with control or RPL11-specific siRNAs and treated with either MLN4924, or with low doses of ActD. MLN4924 causes p53 stabilisation and induction of the well-described p53 regulated gene, Mdm2 (Fig. 4A left, 4B top panel) [35]. However, knockdown of RPL11 reduced p53 stabilisation and transcriptional activation by MLN4924, similar to that observed with ActD (Fig. 4A, B). The defects in p53 stabilisation by MLN4924 were observed with four separate siRNAs, targeting different parts of the RPL11 mRNA sequence (Fig. 4C). Therefore, RPL11 is required for p53 activation by MLN4924, similar to what is observed by ActD-induced nucleolar stress [40, 41].

The Mdm2 E3 ligase is an important p53 regulator, and is known to play a critical role in p53 activation upon nucleolar stress [30, 42]. Direct binding of RPs to Mdm2 blocks Mdm2-mediated p53 degradation allowing p53 accumulation [43]. For RPL11 and RPL5 genetic studies demonstrated the importance of their binding to Mdm2 in p53 nucleolar signaling. Transgenic mice expressing a single amino acid mutant of Mdm2 (C305F) that cannot interact with RPL11 and RPL5 were shown to be resistant to nucleolar stress induced by ActD [44]. To test whether p53 activation by MLN4924 depends on RPL11/RPL5-Mdm2 interaction we used MEFs that express either wild type Mdm2 or the Mdm2 C305F mutant. As reported, low doses of ActD cause p53 stabilisation in the wild type MEFs, but not in the Mdm2 C305F mutant MEFs (Fig. 4D). MLN4924 stabilised p53 in wild type MEFs, although to a much lesser extent than in other cell lines tested. However, in the Mdm2 mutant MEFs, MLN4924 did not cause any detectable p53 stabilization (Fig. 4D, right panel) even though Cullin NEDDylation is completely blocked. Consistent with the above data, knockdown of

RPL5 also compromises MLN4924 induced p53 stabilisation (supplementary information S1). In combination, the above data strongly suggest that MLN4924 causes p53 stabilisation through the nucleolus involving the RP-Mdm2 pathway. We also tested the effect of MLN4924 in the activation of CEP-1, the p53 homologue in *C. elegans*, which lack both key p53 regulators Mdm2 and Mdmx. Treatment of *C. elegans* with either MLN4924 or ActD had no effect on CEP-1/p53 transcriptional activity (Fig. 4E) despite the clear effects on nucleolus size and morphology (Fig. 2C). In contrast, treatment with UV causes a robust CEP-1/p53 activation (Fig. 4E). The data in *C. elegans* recapitulate the results in the transgenic Mdm2C305F mice where p53 is insensitive to nucleolar stress induced by ActD, but not to other forms of DNA damage, due to lack of Mdm2-RP binding [44]. Therefore, lack of nucleolar stress signaling to CEP-1/p53 in *C. elegans* may be due to the absence of Mdm2.

MLN4924 alters the composition of the nucleolar proteome but does not inhibit nucleolar transcription

Comparison between the effects of MLN4924 and ActD within the p53 pathway shows several similarities: Both compounds activate p53 in RPL11/RPL5 and Mdm2C305F dependent manner, inhibit RPL11 NEDDylation and decrease RPL11 nucleolar mobility. The fact that at low doses (1-5nM), ActD is relatively specific in blocking RNA Pol I dependent transcription raises the possibility that MLN4924 can elicit its effect on p53 through transcriptional inhibition in the nucleolus.

We performed different experiments to determine the effect of MLN4924 on nucleolar function. We combined SILAC with mass spectrometry to provide a quantitative proteomic analysis of the nucleolus upon inhibition of NEDDylation [20]. U2OS cells labeled with arginine and lysine containing either light (R0K0), medium (R6K4), or heavy (R10K8) stable isotopes were either untreated [14], or treated with

ActD (medium), or with MLN4924 (heavy), for 15hrs. Equal numbers of light, medium and heavy cells were mixed, fractionated and nucleoli isolated (Fig. 5A). Proteins from the resulting nucleolar extracts were separated by gel filtration and each fraction trypsin digested and analysed by mass spectrometry (supplementary information S2). Over 1,300 proteins were identified and quantified. Treatment with MLN4924 caused an increased abundance of 98 proteins and a decreased abundance of 21 nucleolar proteins by at least 1.3 fold relative to nucleolar proteins of untreated cells (Fig. 5B and supplementary information), whereas low doses of ActD, resulted in 95 nucleolar proteins increasing in abundance and 31 proteins decreasing, by at least 1.5 fold relative to nucleolar protein levels in the untreated control cells (Fig. 5B and supplementary information).

Network analysis for the regulated proteins did not provide any evidence for an effect of MLN4924 on RNA Pol I dependent transcription. Rather, components of the RNA Pol II and DNA replication processes were significantly enriched in the nucleolus upon MLN4924 treatment. This includes elongation activators TCEB1, 2, the component of the core-TFIIH transcription factor GTF2H1, multiple members of the MCM family of DNA replication licensing factors, along with histone acetyltransferase complexes including MRFAP1, MORF4L2 and MORF4L1, Tip60 and the histone de-acetylase HDAC1 (Fig. 5C, S3A, B). The nucleolar abundance of histone H1 and many of its variants was decreased by MLN4924 (S3A, B). Histone H1 is preferentially associated with the "linker" DNA between nucleosomes and is thought not to have a major effect on global transcription but can act as positive or negative gene-specific regulator of transcription in vivo [45]. In contrast and as expected, the major targets of ActD are regulators of RNA Pol I transcriptional activity and rRNA processing including coilin and fibrillarin (S3C). A group of

proteins affected both by MLN4924 and ActD was also identified (Fig. 5D). Interestingly, the relative abundance of RRS1 (Ribosome biogenesis regulatory protein) was decreased following treatment of cells with either compound, while other proteins, such as PCNA (Proliferating cell nuclear antigen) and DNA replication licensing factors, were differentially affected, with MLN4924 increasing and ActD decreasing their nucleolar abundance, respectively. The data indicate that inhibition of NEDDylation causes changes in the nucleolar proteome on a similar scale to the well-described chemotherapeutic drug ActD, but does not affect RNA Pol I function. We further confirmed this notion by directly monitoring the effect of MLN4924 on RNA Pol I activity. We used H1299 cells, which are genetically null for p53, to avoid the potential downstream effects of p53 activation on RNA Pol I transcription [46]. Incorporation of ^{3}H-uridine on nascent rRNA was monitored in H1299 cells treated either with low doses of ActD, or with MLN4924. As expected, ActD caused a dramatic inhibition of 47S rRNA production and in the appearance of the 32S, 28S and 18S rRNA processed forms (Fig. 5E) [25, 47]. However, application of MLN4924 did not cause any detectable changes in rRNA production (Fig. 5E). Consistently, analysis of pre-rRNAs by Northern blotting after MLN4924 treatment did not reveal any major differences for the 40S precursors (5'ITS1 probe) compared to control cells, while ActD treated cells were almost devoid of pre-rRNAs (Fig. 5F). To further investigate the potential effect of MLN4924 on ribosome subunit biogenesis, we analysed ribosome production using sucrose gradient ultracentrifugation. As control we used ActD, which impairs ribosome subunit biogenesis, mainly through inhibition of rRNA production [36]. As expected, ActD caused a decrease in large and small ribosome subunits and polysome formation (Fig. 5G). MLN4924 treatment had no detectable effect on the polysome fraction but it caused a decrease in the ratio of

60S/40S subunit production (Fig. 5G). Similar defects in the 60S/40S ratio have been reported upon knockdown of large ribosome subunit proteins RPL7a, RPL11, RPL5, RPL14, RPL26, RPL35a [48, 49, 50]. The combination of the data, suggest that the activation of p53 by MLN4924 is not due to RNA Pol I inhibition but rather due to re-organisation of the nucleolar proteome that involves targeting RPs.

Differential roles of RPL11 and p53 in MLN4924-induced accumulation of cells in S-phase and cytotoxicity

Our studies have identified RPL11 as an important cellular factor required for the MLN4924 induced p53 activation. The MLN4924 induced toxicity in proliferating cells, is mainly due to the resulting S-phase arrest [11]. We tested the effect of p53 and RPL11 knockdown on cell cycle progression (Fig. 6A, supplementary information S4) and viability (Fig. 6B) upon inhibition of NEDDylation by MLN4924. As expected, treatment of control siRNA transfected MCF7 cells with MLN4924 increased the proportion of cells in S-phase with a corresponding decrease in cell viability (Fig. 6A, 6B). Knockdown of p53 promoted the accumulation of cells in S-phase following MLN4924 treatment and enhanced MLN4924 toxicity (Fig. 6A, 6B). The opposite effect was observed upon RPL11 knockdown, which reduced both the MLN4924-induced accumulation of cells in S-phase and cytotoxicity (Fig. 6A, 6B). However, the effects of RPL11 knockdown on cell cycle and survival are p53 independent, as simultaneous knockdown of RPL11 and p53 did not alter the effect of RPL11 knockdown upon MLN4924 treatment (Fig 6A, 6B). Similar results on cell survival were obtained when instead of MLN4924, siRNAs against the catalytic subunit of NAE (uba3) were used (Fig. 6C).

Thus, our data suggest that while the RPL11-mediated p53 activation by MLN4924 is cytoprotective, loss of RPL11 protects cells against MLN4924 by p53 independent mechanisms.

Discussion

The NEDD8 conjugation pathway controls key cellular processes such as cell viability and cell cycle progression. The promising preclinical studies for inhibitors of NEDDylation have emphasized the importance of the NEDD8 pathway as a novel drug target. Therefore, elucidation of pathways that are controlled by NEDDylation is critical for our understanding of the mechanisms of action for these potential new chemotherapeutics. The MLN4924-induced activation of p53 is relevant to the cellular response to MLN4924 treatment, albeit the mechanism remains elusive. In this study, we show that MLN4924 activates the p53 tumour suppressor through the RP-Mdm2 pathway with characteristics of nucleolar stress. One of the pleiotropic effects of MLN4924 is to alter the morphology and to increase the size of the nucleolus. Similar effects on nucleolus size were observed in germline cells of MLN4924 treated *C. elegans*, which suggests a highly conserved role for protein NEDDylation to control the function of the nucleolus.

Changes in nucleolar size and morphology are associated with changes in rates of proliferation. Indeed, nucleolar hypertrophy is linked to malignancy, as increase in Pol I activity and ribosome production is required to sustain higher rates of growth [51]. Reduction in nucleolar size or fragmentation is linked with the action of chemotherapeutics such as ActD, which inhibit Pol I function and cause cell cycle arrest [24, 28]. In the contrary, we found that MLN4924, a compound with anti-proliferative effects, increases nucleolar size indicating that nucleolar hypertrophy may not always be associated to higher rates of cell growth.

Quantitative proteomics showed that the MLN4924-induced morphological changes in the nucleolus are associated with a re-organisation of the nucleolar proteome that are of similar scale to the well-described nucleolar "stressor" ActD. However, a key

difference compared to ActD, is that MLN4924 does not affect rRNA production/processing. Interestingly, MLN4924 increases the nucleolar abundance of multiple members of the MCM family of DNA replication licensing factors, along with histone acetyltransferase complexes, which are essential for DNA replication licensing [52, 53] (supplementary information S3). Indeed, we found that the replication factor MCM2 is relocalised to the peri-nucleolar area upon MLN4924 treatment (supplementary information S5). Therefore, the increase in nucleolar size by MLN4924 may be associated to the increase in the abundance of replication [54] and acetylation factors either within the nucleolus or as nucleolar-associated proteins.

Although the effects of MLN4924 and ActD on nucleolar function are different the downstream signaling events that lead to p53 activation are quite similar. Both compounds inhibit RPL11-NEDDylation and reduce the mobility of RPL11 in the nucleolus. Furthermore, the p53 activation induced by either compound depends on the interaction of RPL11/RPL5 with Mdm2, which is regarded as a key step in p53 activation specifically upon nucleolar stress and not upon DNA damage [44]. Therefore, despite the pleiotropic effects induced due to inhibition of CRL function, p53 activation by MLN4924 depends strictly on the RP-Mdm2 module. We propose that MLN4924 causes "nucleolar stress" by affecting the nucleolar proteome rather than inhibiting nucleolar transcription. The downstream biological outcome is the signaling to cell cycle regulators such as p53 that depends on the RP-Mdm2 pathway. Interestingly, combination of MLN4924 with ActD provides an additive effect on p53 stabilisation, indicating that these compounds act on the same signaling pathway (supplementary information S6). This further supports the notion that MLN4924 activates p53 through nucleolar signaling, most likely downstream of PolI activity regulation and upstream of the RP-Mdm2 module. While our studies suggest that

NEDDylation of RPL11 is a target of MLN4924, we cannot exclude the possibility that the observed changes in the nucleolar proteome and resulting p53 activation is indirectly due to CRL inhibition.

The nucleolus is viewed as a major hub for the detection of cellular stress, which elicits signaling events that control the activity of tumour suppressors and oncogenes [24]. The placticity and highly dynamic nature of the nucleolar proteome is a major determinant of decoding a stress signal to a signaling output [23]. The changes in the nucleolar proteome upon stress conditions are directly linked to the regulation of key components of the cell cycle [23, 29]. To our knowledge MLN4924 is the first example of a small compound that re-organises the nucleolar proteome and activates p53 with all the characteristics of "nucleolar stress" in the absence of inhibition of nucleolar transcription. The data suggest that targeting the nucleolar proteome may elicit the required signaling events to cell cycle regulators without affecting rRNA production and ribosome biosynthesis. This may be important as targetting Pol I activity is emerging as an attractive anti cancer approach [55, 56, 57].

Intriguingly, neither MLN4924 nor ActD caused transcriptional activation of CEP-1/p53 in *C. elegans* despite their clear effects on nucleolar morphology and size (Fig. 3A, C, 5E). Previous studies in *C.elegans* showed that depletion of the nucleolar RNA-associated protein NOL-6 induces immunity against bacteria infection through activation of CEP-1/p53, suggesting that the nucleolus can signal to CEP-1/p53 under stress conditions [58]. A homologue for Mdm2 has not been found in nematodes so it is possible that MLN4924 and ActD induced p53 activation depends strictly on the Mdm2 presence, whereas NOL-6 induced signaling depends on other E3-ligases or other mechanisms of CEP-1/p53 activity regulation (translational) [59].

While p53 activation by MLN4924 depends on RPL11, cell cycle analysis and survival assays show a differential role for p53 and RPL11 in the MLN4924 response. Our data are consistent with previous studies showing that the MLN4924 induced activation of p53 is cytoprotective [13]. This is most likely due to the p53 induced G1 arrest that prevents entry of cells in the S-phase where MLN4924 elicits toxicity. In contrary, RPL11 is required for the MLN4924-induced accumulation of cells in S-phase and cytotoxicity. However, these effects are p53 independent, indicating that additional pathways controlled by RPL11 are involved in the MLN4924 biological response. For example, RPL11 controls the transcriptional activity of c-myc and cyclin expression [60,61,62]. Indeed, loss of RPL11 was shown to suppress cell proliferation, in the absence of cell cycle arrest, independently of p53 [62]. The data also indicate that the rates of cell proliferation may be a critical determinant for the effectiveness of MLN4924 as potential chemotherapeutic.

In summary, the present study shows that MLN4924 activates p53 through the RP-Mdm2 pathway and suggests that targeting the nucleolus is, at least in part, a mechanism of action for inhibitors of NEDDylation.

Materials and Methods

Gene expression

RNA from MCF7 cells transfected with siRNAs and treated with ActD or MLN4924 was isolated and used for cDNA synthesis. The cDNA was then used for quantitative real-time PCR (qRT-PCR) to monitor mdm2 expression. Primers for mdm2 (P2) promoter were previously described [63]. Full details can be found in supplementary information.

Isolation of His_6-NEDDylated proteins, ribosome profiling

Ni^{2+}-pull downs and total cell extracts were prepared as described in [64, 65]. Ribosome profiling was performed as described in [36].

Detection of newly synthesised RNA and rRNA processing

Transcription efficiency was monitored by ^{3}H-uridine incorporation of newly synthesized RNAs as described [66]. Briefly, H1299 cells were treated with ActD or MLN4924 and pulsed with ^{3}H-uridine for 1hr at 37^{o}C. RNA was isolated and subjected to agarose-formaldehyde gel electrophoresis. For monitoring rRNA processing, H1299 cells were treated as above for 8 or 15hrs and isolated total RNA was used for northern blotting with ^{32}P-labelled probes to reveal either all 18S precursors (5'ITS1) or 28S and 5.8S (ITS2). Full details can be found in supplementary information.

Microscopy

FRAP experiments were performed in H1299 cells stably expressing RPL11-EGFP as described in [35]. Details are included in supplementary information. For immunostaining in U2OS cells, samples were prepared and methods were used as described in [67]. All primary antibodies were used at 1:100 dilution.

Flow cytometry

MCF7 cells in 6 well plates were transfected with 5nM control, RPL11 and p53 siRNAs as indicated. The total amount of siRNAs was normalised to 10nM with control siRNA. 48hrs post transfection cells were treated with either DMSO or with MLN4924 (0.5μM) for 24hrs. Cells were collected by trypsin, fixed with ethanol at 4^{o}C and labelled with propidium iodide for 30min. DNA content of 10,000 cells per condition was quantified on a FACS Calibur (Becton Dickinson) using Cell Quest acquisition software and employing pulse-width analysis to exclude doublets. Data were analysed using Flowjo software (Treestar Inc) and the Watson (pragmatic) model to determine cell cycle distribution.

Treatments

For each experiments of drug assay, 500 worms were treated at L4 larval stage in liquid culture of M9 medium complemented with cholesterol (5μg/ml) and HT115 bacteria ($4x10^5$). MLN4924 was used at 100μM, Actinomycin D at 100nM and Doxorubicin at 100μM. Compounds were diluted in M9 solution before use. For UV response L4 worms were exposed at 100J/m^2 and dissected 5 hours later. After treatment of MLN4924 or ActD, worms were dissected or put in trizol for qRT-PCR.

Nucleoli volume quantification with Image J software

Observations were performed using Zeiss Axioimager Z2. For each germline, pachytene stage was observed with 63x objective and stacks of all the thickness were obtained (0.5μm/stack) to see overall nucleus with Metamorph software. The same stack representing the nucleus (DAPI staining) and the nucleolus (Fibrillarin staining) was selected for further analysis. An average of 50 nuclei in human cells and 6

germlines-50 nuclei in *C. elegans* were used for each experiment. Full details can be found in supplementary information.

Subcellular fractionation and proteomics.

DMEM media depleted of arginine (R) and lysine (K) were supplemented with 10% dialysed FCS and either light (K0R0), medium (K4R6) or heavy (K8R10) labelled amino acids. U2OS cells were grown in different media and after 6 passages full incorporation was confirmed. 20x15cm dishes for each condition were grown till 80% confluency before treatment. Subcellular fractionation and isolation of nucleoli was performed as described in [20] and supplementary information.

Survival assays

MCF7 cells were seeded and transfected with 5nM of each of the siRNA pool in 24-well plates (15000 cells/well). The total amount of siRNAs was normalised to 10nM with control siRNA. 24 hrs later, MLN4924 was added for the indicated periods before cell survival was measured with the CellTiter-Glo Luminescence assay from Promega according to manufacturer's instructions. In each transfection (Fig. 6B), DMSO was added in control cells for 72 hrs.

Potential conflict of interest: P.S. was an employee of Millennium Pharmaceuticals at the start of the studies.

Acknowledgments

We are grateful to Dr Yanping Zhang for providing the wild type and mutant Mdm2 C305F MEFs, the Montpellier RIO Imaging facility and Stefano Fumagalli for critical reading of the manuscript.

References

1 Abidi N, Xirodimas DP. Regulation of cancer-related pathways by protein NEDDylation and strategies for the use of NEDD8 inhibitors in the clinic. *Endocr Relat Cancer* 2015; **22**: T55-70.

2 Enchev RI, Schulman BA, Peter M. Protein neddylation: beyond cullin-RING ligases. *Nat Rev Mol Cell Biol.* 2014; **16**: 30-44.

3 Watson IR, Irwin MS, Ohh M. NEDD8 pathways in cancer, Sine Quibus Non. *Cancer Cell* 2011; **19**: 168-176.

4 Wang M, Medeiros BC, Erba HP, DeAngelo DJ, Giles FJ, Swords RT. Targeting protein neddylation: a novel therapeutic strategy for the treatment of cancer. *Expert Opin Ther Targets* 2011; **15**: 253-264.

5 Liakopoulos D, Doenges G, Matuschewski K, Jentsch S. A novel protein modification pathway related to the ubiquitin system. *EMBO J* 1998; **17**: 2208-2214.

6 Osaka F, Kawasaki H, Aida N, Saeki M, Chiba T, Kawashima S *et al*. A new NEDD8-ligating system for cullin-4A. *Genes Dev* 1998; **12**: 2263-2268.

7 Petroski MD, Deshaies RJ. Function and regulation of cullin-RING ubiquitin ligases. *Nat Rev Mol Cell Biol* 2005; **6**: 9-20.

8 Duda DM, Scott DC, Calabrese MF, Zimmerman ES, Zheng N, Schulman BA. Structural regulation of cullin-RING ubiquitin ligase complexes. *Curr Opin Struct Biol 2011*; **21**: 257-264.

9 Harper JW, Tan MK. Understanding cullin-RING E3 biology through proteomics-based substrate identification. *Mol Cell Proteomics* 2012; **11**: 1541-1550.

10 Duncan K, Schafer G, Vava A, Parker MI, Zerbini LF. Targeting neddylation in cancer therapy. *Future Oncol* 2012; **8**: 1461-1470.

11 Soucy TA, Smith PG, Milhollen MA, Berger AJ, Gavin JM, Adhikari S *et al*. An inhibitor of NEDD8-activating enzyme as a new approach to treat cancer. *Nature* 2009; **458**: 732-736.

12 Brownell JE, Sintchak MD, Gavin JM, Liao H, Bruzzese FJ, Bump NJ *et al*. Substrate-assisted inhibition of ubiquitin-like protein-activating enzymes: the NEDD8 E1 inhibitor MLN4924 forms a NEDD8-AMP mimetic in situ. *Mol Cell* 2010; **37**: 102-111.

13 Lin JJ, Milhollen MA, Smith PG, Narayanan U, Dutta A. NEDD8-targeting drug MLN4924 elicits DNA rereplication by stabilizing Cdt1 in S phase,

triggering checkpoint activation, apoptosis, and senescence in cancer cells. *Cancer Res* 2010; **70**: 10310-10320.

14 Blank JL, Liu XJ, Cosmopoulos K, Bouck DC, Garcia K, Bernard H *et al*. Novel DNA damage checkpoints mediating cell death induced by the NEDD8-activating enzyme inhibitor MLN4924. *Cancer Res* 2013; **73**: 225-234.

15 Lempiainen H, Shore D. Growth control and ribosome biogenesis. *Curr Opin Cell Biol* 2009; **21**: 855-863.

16 Kressler D, Hurt E, Bassler J. Driving ribosome assembly. *Biochim Biophys Acta* 2010; **1803**: 673-683.

17 Montanaro L, Trere D, Derenzini M. Nucleolus, ribosomes, and cancer. *Am J Pathol* 2008; **173**: 301-310.

18 Andersen JS, Lyon CE, Fox AH, Leung AK, Lam YW, Steen H *et al*. Directed proteomic analysis of the human nucleolus. *Curr Biol* 2002; **12**: 1-11.

19 Fox AH, Lam YW, Leung AK, Lyon CE, Andersen J, Mann M *et al*. Paraspeckles: a novel nuclear domain. *Curr Biol* 2002; **12**: 13-25.

20 Andersen JS, Lam YW, Leung AK, Ong SE, Lyon CE, Lamond AI *et al*. Nucleolar proteome dynamics. *Nature* 2005; **433**: 77-83.

21 Hernandez-Verdun D. Nucleolus: from structure to dynamics. *Histochem Cell Biol* 2006; **125**: 127-137.

22 Greco A. Involvement of the nucleolus in replication of human viruses. *Rev Med Virol* 2009; **19**: 201-214.

23 Boulon S, Westman BJ, Hutten S, Boisvert FM, Lamond AI. The nucleolus under stress. *Mol Cell* 2010; **40**: 216-227.

24 Rubbi CP, Milner J. Disruption of the nucleolus mediates stabilization of p53 in response to DNA damage and other stresses. *EMBO J* 2003; **22**: 6068-6077.

25 Perry RP, Kelley DE. Inhibition of RNA synthesis by actinomycin D: characteristic dose-response of different RNA species. *J Cell Physiol* 1970; **76**: 127-139.

26 Donati G, Peddigari S, Mercer CA, Thomas G. 5S ribosomal RNA is an essential component of a nascent ribosomal precursor complex that regulates the Hdm2-p53 checkpoint. *Cell Rep* 2013; **4**: 87-98.

27 Horn HF, Vousden KH. Cooperation between the ribosomal proteins L5 and L11 in the p53 pathway. *Oncogene* 2008; **27**: 5774-5784.

28 Vlatkovic N, Boyd MT, Rubbi CP. Nucleolar control of p53: a cellular Achilles' heel and a target for cancer therapy. *Cell Mol Life Sci* 2014; **71**: 771-791.

29 Golomb L, Volarevic S, Oren M. p53 and ribosome biogenesis stress: The essentials. *FEBS Lett* 2014; **588**: 2571-2579.

30 Zhang Y, Lu H. Signaling to p53: ribosomal proteins find their way. *Cancer Cell* 2009; **16**: 369-377.

31 Lindstrom MS. Emerging functions of ribosomal proteins in gene-specific transcription and translation. *Biochem Biophys Res Commun* 2009; **379**: 167-170.

32 Baker NE. Developmental regulation of nucleolus size during Drosophila eye differentiation. *PLoS One* 2013; **8**: e58266.

33 Lee LW, Lee CC, Huang CR, Lo S J. The nucleolus of Caenorhabditis elegans. *J Biomed Biotechnol* 2012; 601274.

34 Sundqvist A, Liu G, Mirsaliotis A, Xirodimas DP. Regulation of nucleolar signalling to p53 through NEDDylation of L11. *EMBO Rep* 2009; **10**: 1132-1139.

35 Barak Y, Juven T, Haffner R, Oren M. mdm2 expression is induced by wild type p53 activity. *EMBO J* 1993; **12**: 461-468.

36 Xirodimas DP, Sundqvist A, Nakamura A, Shen L, Botting C, Hay RT. Ribosomal proteins are targets for the NEDD8 pathway. *EMBO Rep* 2008; **9**: 280-286.

37 Chen D, Huang S. Nucleolar components involved in ribosome biogenesis cycle between the nucleolus and nucleoplasm in interphase cells. *J Cell Biol* 2001; 153; 169-176.

38 Olson MO, Dundr M. The moving parts of the nucleolus. Histochem Cell Biol 2005; **123**: 203-216.

39 Lam YW, Lamond AI, Mann M, Andersen JS. Analysis of nucleolar protein dynamics reveals the nuclear degradation of ribosomal proteins. *Curr Biol* 2007; **17**: 749-760.

40 Lohrum MA, Ludwig RL, Kubbutat MH, Hanlon M, Vousden KH. Regulation of HDM2 activity by the ribosomal protein L11. *Cancer Cell* 2003; **3**: 577-587.

41 Zhang Y, Wolf GW, Bhat K, Jin A, Allio T, Burkhart WA *et al*. Ribosomal protein L11 negatively regulates oncoprotein MDM2 and mediates a p53-dependent ribosomal-stress checkpoint pathway. *Mol Cell Biol* 2003; **23**: 8902-8912.

42 Kruse JP, Gu W. Modes of p53 regulation. *Cell* 2009; **137**: 609-622.

43 Lindstrom MS, Jin A, Deisenroth C, White Wolf G, Zhang Y. Cancer-associated mutations in the MDM2 zinc finger domain disrupt ribosomal protein interaction and attenuate MDM2-induced p53 degradation. *Mol Cell Biol* 2007; **27**: 1056-1068.

44 Macias E, Jin A, Deisenroth C, Bhat K, Mao H, Lindstrom MS *et al*. An ARF-independent c-MYC-activated tumor suppression pathway mediated by ribosomal protein-Mdm2 Interaction. *Cancer Cell* 2010; **18**: 231-243.

45 Shen X, Gorovsky MA. Linker histone H1 regulates specific gene expression but not global transcription in vivo. *Cell* 1996; **86**: 475-483.

46 White RJ. RNA polymerases I and III, non-coding RNAs and cancer. *Trends Genet* 2008; **24**: 622-629.

47 Sobell HM. Actinomycin and DNA transcription. *Proc Natl Acad Sci U S A* 1985; **82**: 5328-5331.

48 Robledo S, Idol RA, Crimmins DL, Ladenson JH, Mason PJ, Bessler M. The role of human ribosomal proteins in the maturation of rRNA and ribosome production. *RNA* 2008; **14**: 1918-1929.

49 Fumagalli S, Di Cara A, Neb-Gulati A, Natt F, Schwemberger S, Hall J *et al*. Absence of nucleolar disruption after impairment of 40S ribosome biogenesis reveals an rpL11-translation-dependent mechanism of p53 induction. *Nat Cell Biol* 2009; **11**: 501-508.

50 Fumagalli S, Ivanenkov VV, Teng T, Thomas G. Suprainduction of p53 by disruption of 40S and 60S ribosome biogenesis leads to the activation of a novel G2/M checkpoint. *Genes Dev* 2012; **26**: 1028-1040.

51 Derenzini M, Montanaro L, Trere D. What the nucleolus says to a tumour pathologist. *Histopathology* 2009; **54**: 753-762.

52 Chadha GS, Blow JJ. Histone acetylation by HBO1 tightens replication licensing. *Mol Cell* 2010; **37**: 5-6.

53 Miotto B, Struhl K. HBO1 histone acetylase activity is essential for DNA replication licensing and inhibited by Geminin. *Mol Cell* 2010; **37**: 57-66.

54 Larance M, Kirkwood KJ, Xirodimas DP, Lundberg E, Uhlen M, Lamond AI. Characterization of MRFAP1 turnover and interactions downstream of the NEDD8 pathway. *Mol Cell Proteomics* 2012; **11**: M111 014407.

55 Hannan RD, Drygin D, Pearson RB. Targeting RNA polymerase I transcription and the nucleolus for cancer therapy. *Expert Opin Ther Targets* 2013; **17**: 873-878.

56 Drygin D, O'Brien SE, Hannan RD, McArthur GA, Von Hoff DD. Targeting the nucleolus for cancer-specific activation of p53. *Drug Discov Today* 2014; **19**: 259-265.

57 Bywater MJ, Poortinga G, Sanij E, Hein N, Peck A, Cullinane C *et al*. Inhibition of RNA polymerase I as a therapeutic strategy to promote cancer-specific activation of p53. *Cancer Cell* 2012; **22**: 51-65.

58 Fuhrman LE, Goel AK, Smith J, Shianna KV, Aballay A. Nucleolar proteins suppress Caenorhabditis elegans innate immunity by inhibiting p53/CEP-1. *PLoS Genet* 2009; **5**: e1000657.

59 James A, Wang Y, Raje H, Rosby R, DiMario P. Nucleolar stress with and without p53. *Nucleus* 2014; **5**: 402-26

60 Sun XX, Wang YG, Xirodimas DP, Dai MS. Perturbation of 60 S ribosomal biogenesis results in ribosomal protein L5- and L11-dependent p53 activation. *J Biol Chem* 2010; **285**: 25812-25821.

61 Dai MS, Arnold H, Sun XX, Sears R, Lu H. Inhibition of c-Myc activity by ribosomal protein L11. *EMBO J* 2007; **26**: 3332-3345.

62 Teng T, Mercer CA, Hexley P, Thomas G, Fumagalli S. Loss of tumor suppressor RPL5/RPL11 does not induce cell cycle arrest but impedes proliferation due to reduced ribosome content and translation capacity. *Mol Cell Biol*. 2013; **33**:4660-71.

63 Saville MK, Sparks A, Xirodimas DP, Wardrop J, Stevenson LF, Bourdon JC *et al*. Regulation of p53 by the ubiquitin-conjugating enzymes UbcH5B/C in vivo. *J Biol Chem* 2004; **279**: 42169-42181.

64 Xirodimas D, Saville MK, Edling C, Lane DP, Lain S. Different effects of p14ARF on the levels of ubiquitinated p53 and Mdm2 in vivo. *Oncogene* 2001; **20**: 4972-4983.

65 Tatham MH, Rodriguez MS, Xirodimas DP, Hay RT. Detection of protein SUMOylation in vivo. *Nat Protoc* 2009; **4**: 1363-1371.

66 Pestov DG, Lapik YR, Lau LF. Assays for ribosomal RNA processing and ribosome assembly. *Curr Protoc Cell Biol* 2008; **Chapter 22**: Unit 22 11.

67 Liu G, Xirodimas DP. NUB1 promotes cytoplasmic localization of p53 through cooperation of the NEDD8 and ubiquitin pathways. *Oncogene* 2010; **29**: 2252-2261.

Figure Legends

Figure 1

(A) H1299 cells were treated either with DMSO (control) or with MLN4924 (1μM) for 24hrs. Phase contrast micrographs were then taken and arrows indicate the position of nucleoli. (B) U2OS cells were treated with DMSO or MLN4924 (1μM, 15hrs) before staining for nucleolin, fibrillarin or B23. (C) U2OS cells were treated as above for 24 hrs before cells were fixed and stained for fibrillarin to define the nucleolus and with DAPI to define the nucleus. The relative surface of the nucleoli was determined as described in supplementary information. (D) Quantitation of data represented as relative changes in surface size of the nucleolus (nucleolus/nucleus). (E) U2OS cells were treated with DMSO, ActD (5nM) or doxorubicin (1μM) for 24hrs before fixing and staining for fibrillarin as in (A, C).

Figure 2

(A) *C. elegans* L4 adults were treated with DMSO or with MLN4924 (100μM for 24hrs) or fed with NED-8 RNAi bacteria. The germlines were then dissected and stained for fibrillarin and DAPI as in Fig. 1. (B) The surface size of the nucleolus was determined as in Fig 1D. (C) In the experiment performed in A, animals were also treated with 100J/m^2, or ActD (100nM) or doxorubicin (100μM) as described in materials and methods.

Figure 3

(A) MCF7 cells were treated with MLN4924 at the indicated doses for 24 hrs. Cells were lysed in 2xSDS buffer and extracts were analysed by western blotting. Equal loading was monitored with β-actin. (B) H1299 cells were transfected with His_6-NEDD8 (2μg), Flag-L11 (5μg). 24 hrs post-transfection cells were treated with

MLN4924 (1μM) for the indicated times before cells were harvested. NEDDylated proteins and total cell extracts were prepared as described in material and methods and analysed by western blotting with the appropriate antibodies. Signals for NEDD8-L11 and total L11 were quantified using Image Gauge. Changes in absolute L11-NEDDylation upon MLN4924 treatment were determined by the ratio of NEDDylated over total L11. (C) H1299 cells stably expressing RPL11-EGFP were treated for 4hrs with DMSO, ActD (5nM) or MLN4924 (1μM) before the FRAP experiment. The half-life of recovery (bottom left) and the mobile fraction (bottom right) were calculated as described in materials and methods.

Figure 4

(A) MCF7 cells were transfected with either control or RPL11 siRNAs in duplicates, before treated with MLN4924 (1μM, left panel) or ActD (5nM, right panel) as indicated. Cell extracts and western blot analysis was performed as in Fig.1. (B) Experiment performed as in (A) for the indicated time points and mRNA was isolated as described in Materials and Methods. Expression of the mdm2 gene was monitored by qPCR. Expression of actin was used to normalise the values. Data are represented as mean values +/- standard deviations from 3 independent experiments. (C) Experiment performed as in (A) with individual siRNAs against different parts of RPL11 sequence and treating cells with MLN4924 as indicated. (D) Wild type MEFs or MEFs expressing the Mdm2C305F mutant were treated with ActD (5nM) or MLN4924 (1μM) as indicated. Cell extracts were analysed by western blotting for the indicated proteins (E) *C. elegans* L4 adults were treated as indicated before expression of egl-1 was determined by qPCR. For UV, expression was determined 5hrs post treatment and 24hrs post chemical treatment.

Figure 5

(A) Strategy for SILAC labelling in U2OS cells and proteomic analysis of nucleoli. (B) Profile of nucleolar proteins affected by MLN4924 or ActD. (C) Bioinformatic analysis using Panther software illustrating biological processes affected by MLN4924 and ActD. (D) Proteins affected both by MLN4924 and ActD. (E) H1299 cells were pre-treated with DMSO (5hrs), ActD (5nM) or MLN4924 (1μM) as indicated in duplicates and one set of cells was used for labelling for 1hr with ^{3}H-uridine and monitoring of rRNA production. EtBr staining was used to monitor loading of total RNA. The other set of cells was used for lysis in 2xSDS lysis buffer and western blot analysis (low panel). (F) H1299 cells were treated as above for 8 or 15 hrs. rRNA processing was monitored with the indicated probes as described in methods. (G) H1299 cells were treated as above for 15hrs. Cells were harvested and extracts were used for ribosome profiling as described in methods.

Figure 6

MCF7 cells were transfected with either control, RPL11 and p53 siRNAs as indicated. 48hrs post-transfection cells were treated with DMSO or with MLN4924 (0.5μM) for 24hrs before cell cycle analysis. Histograms show the cell cycle profiles and % of cell populations in different phases. (B) MCF7 cells were transfected with the indicated siRNAs and 24hrs later cells were exposed to MLN4924 (1μM) for 24, 48 or 72hrs. For each siRNA experiment, survival was normalised against the control treated (DMSO) cells, represented as 100%. (C) To mimic the experiment performed in B using MLN4924, siRNA against the catalytic subunit of NAE was used in combination with RPL11 and p53 siRNAs as indicated. Cell survival was measured 72hrs later and values are presented as percentage changes over the control siRNA

transfected cells. For experiments in B and C, data presented the average of 3 independent experiments +/- standard deviations.

Figure 1

A

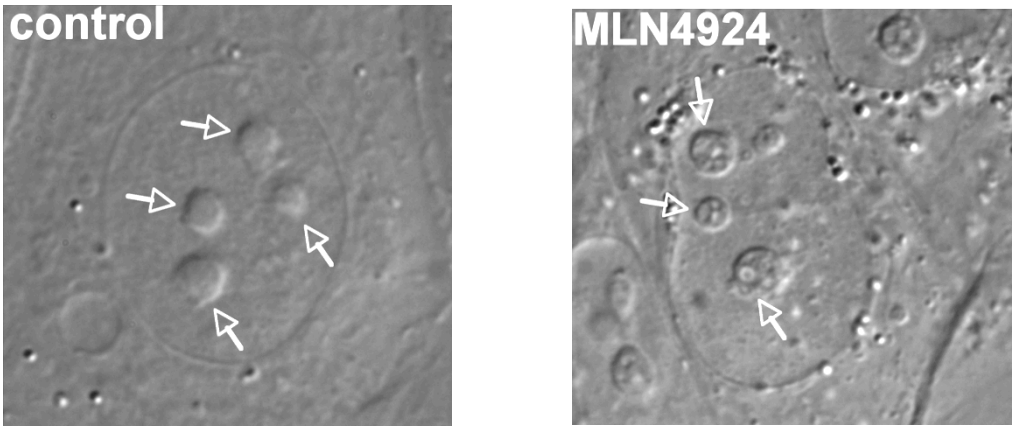

B

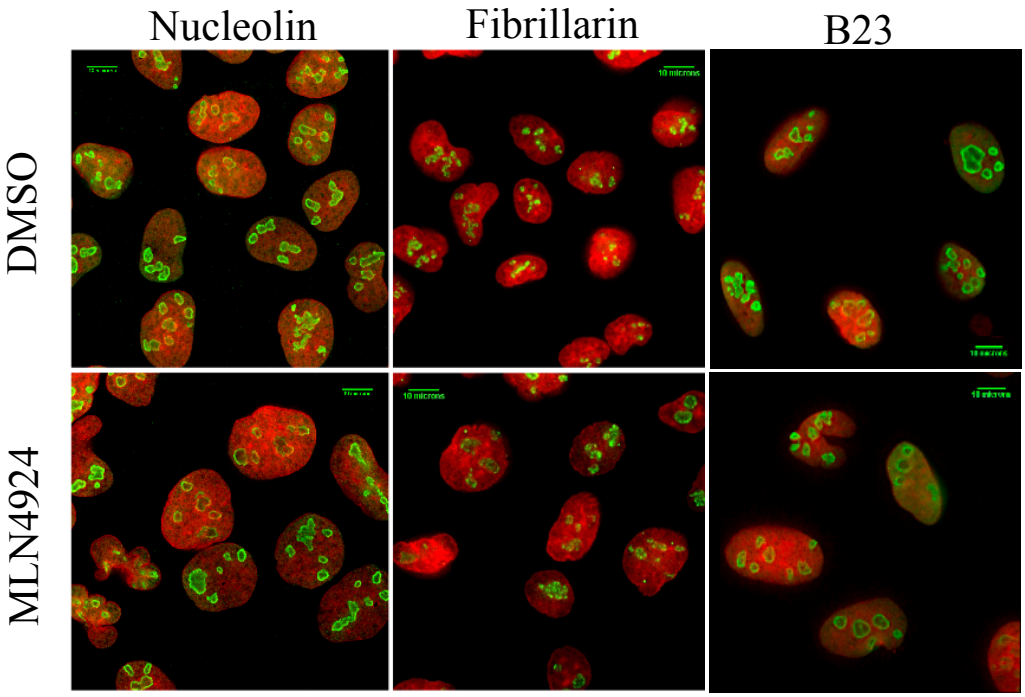

Figure 1

C

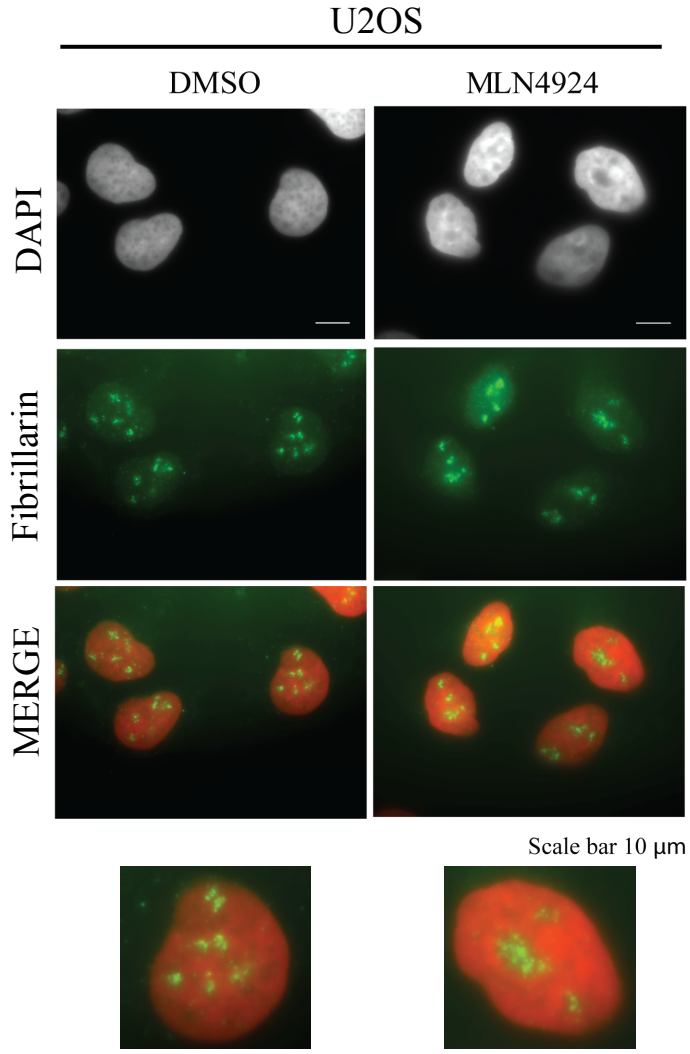
U2OS
DMSO
MLN4924
DAPI
Fibrillarin
MERGE
Scale bar 10 µm

D

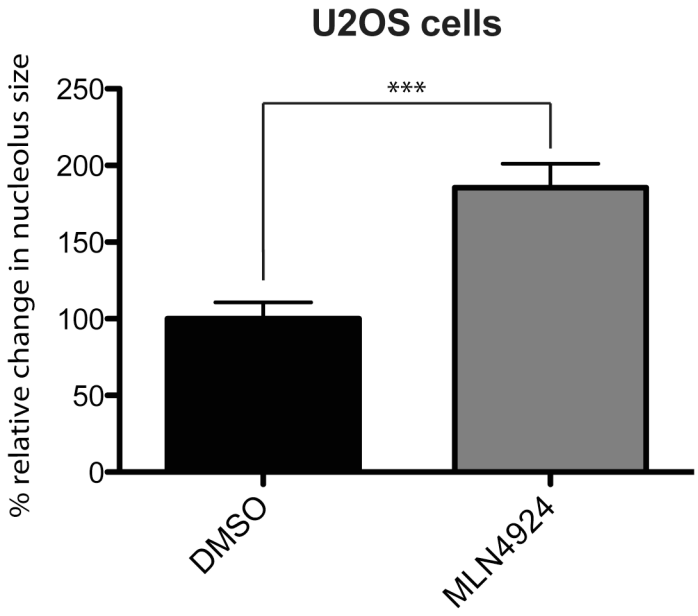
U2OS cells
% relative change in nucleolus size
250
200
150
100
50
0
***
DMSO
MLN4924

Figure 1

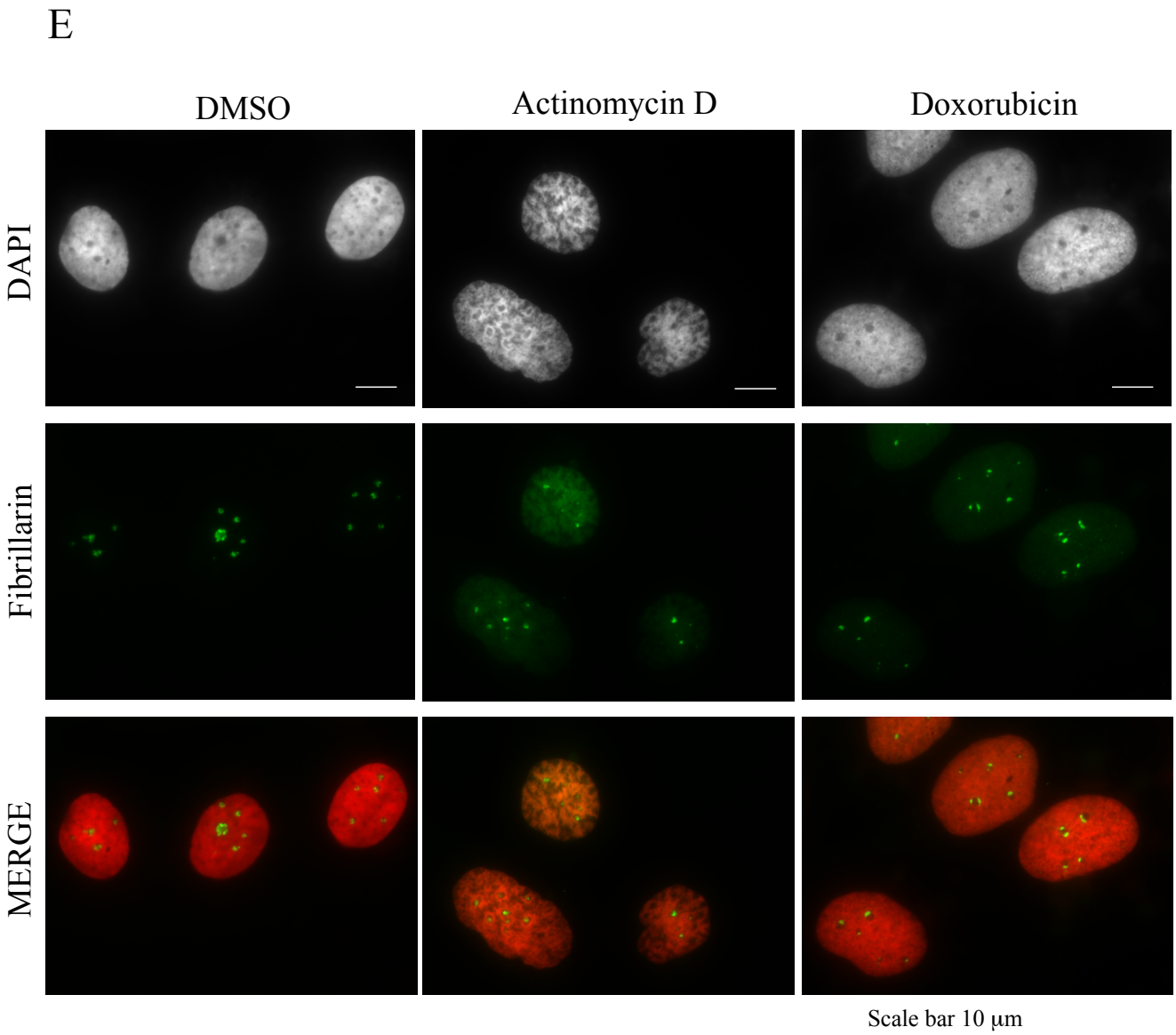
E
DMSO
Actinomycin D
Doxorubicin
DAPI
Fibrillarin
MERGE
Scale bar 10 μm

Figure 2

A

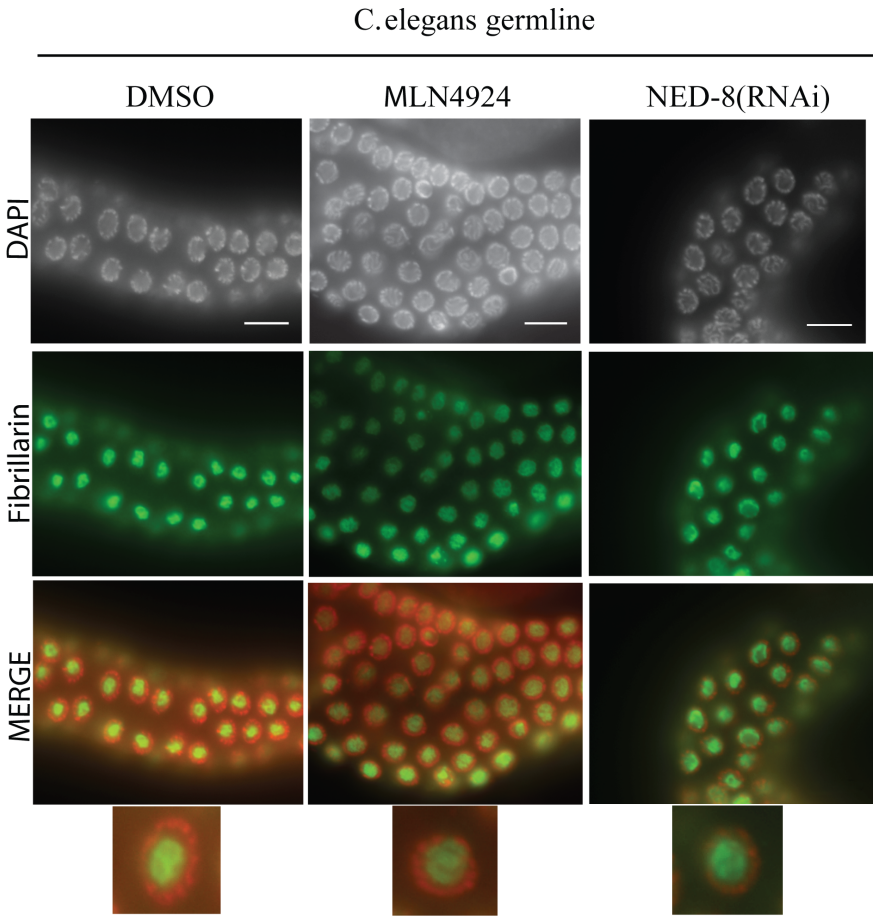
C.elegans germline
DMSO
MLN4924
NED-8(RNAi)
DAPI
Fibrillarin
MERGE

B

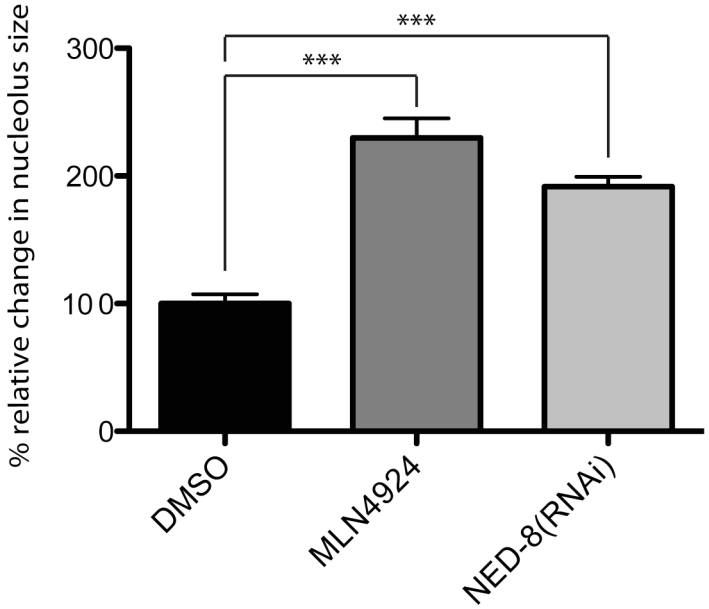
% relative change in nucleolus size
300
200
100
0
***
***
DMSO
MLN4924
NED-8(RNAi)

Figure 2

C

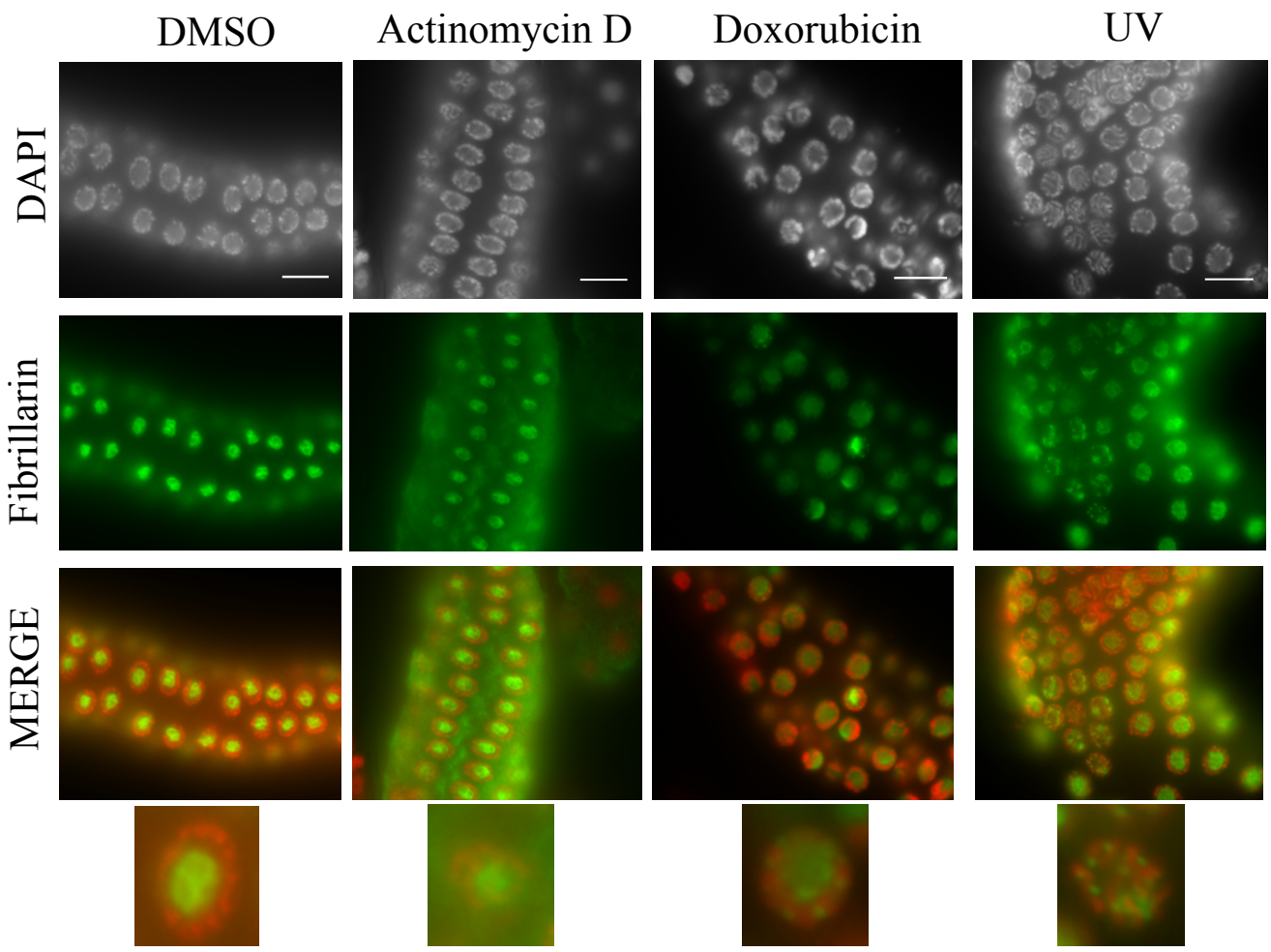

Scale bar 10uM

Figure 3

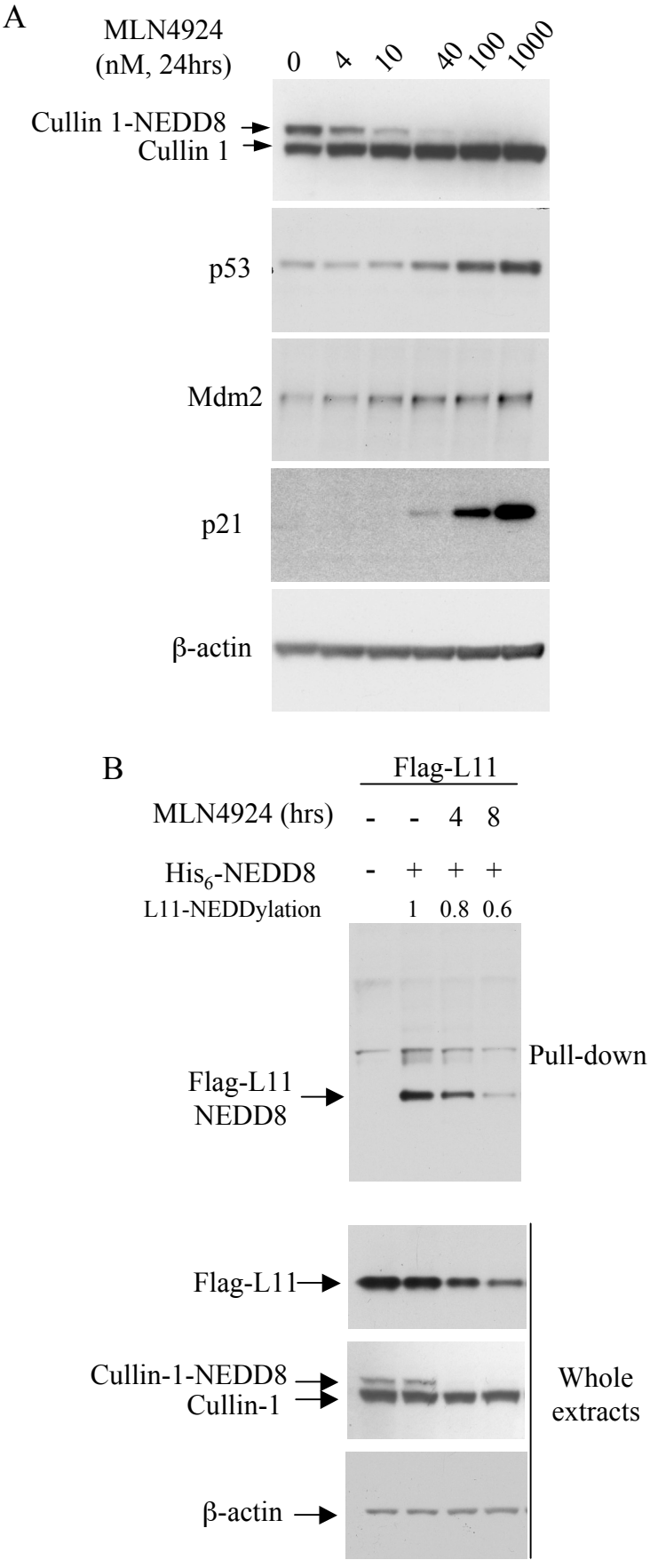
A
MLN4924
(nM, 24hrs)
0
4
10
40
100
1000
Cullin 1-NEDD8
Cullin 1
p53
Mdm2
p21
β-actin
B
Flag-L11
MLN4924 (hrs)
- - 4 8
His6-NEDD8
- + + +
L11-NEDDylation
1 0.8 0.6
Flag-L11
NEDD8
Pull-down
Flag-L11
Cullin-1-NEDD8
Cullin-1
β-actin
Whole
extracts

Figure 3

C

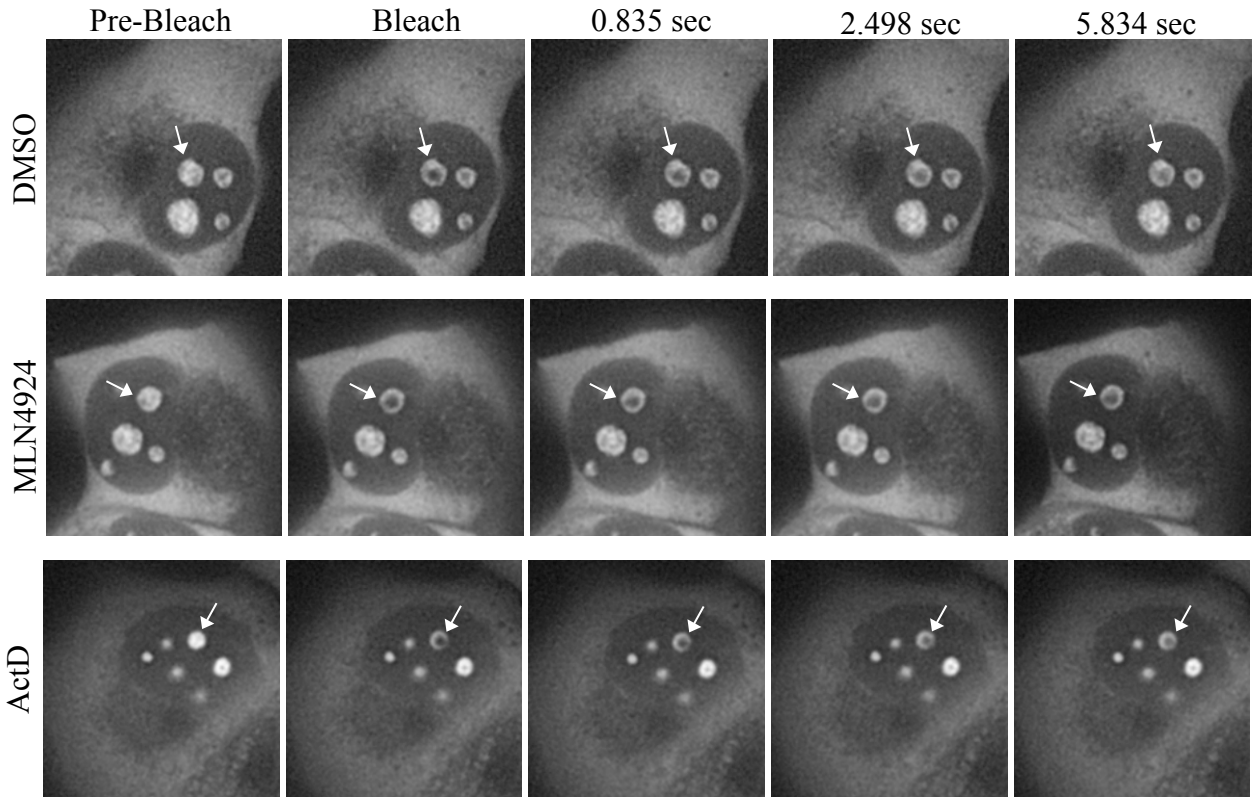

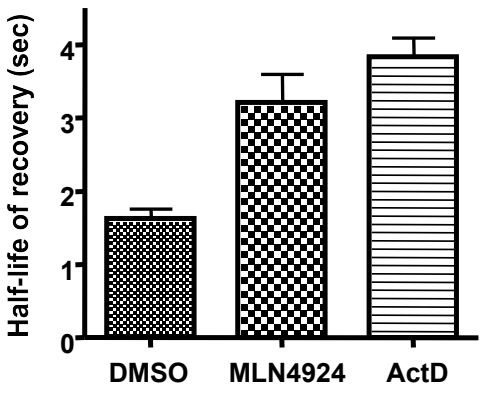

***P < 0.0001, n=20

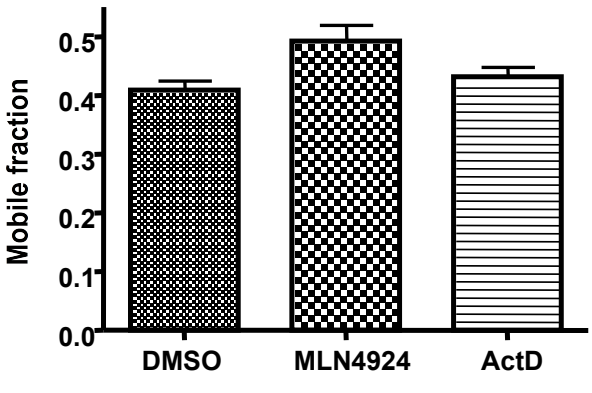

***P < 0.0001, n=20

Figure 4

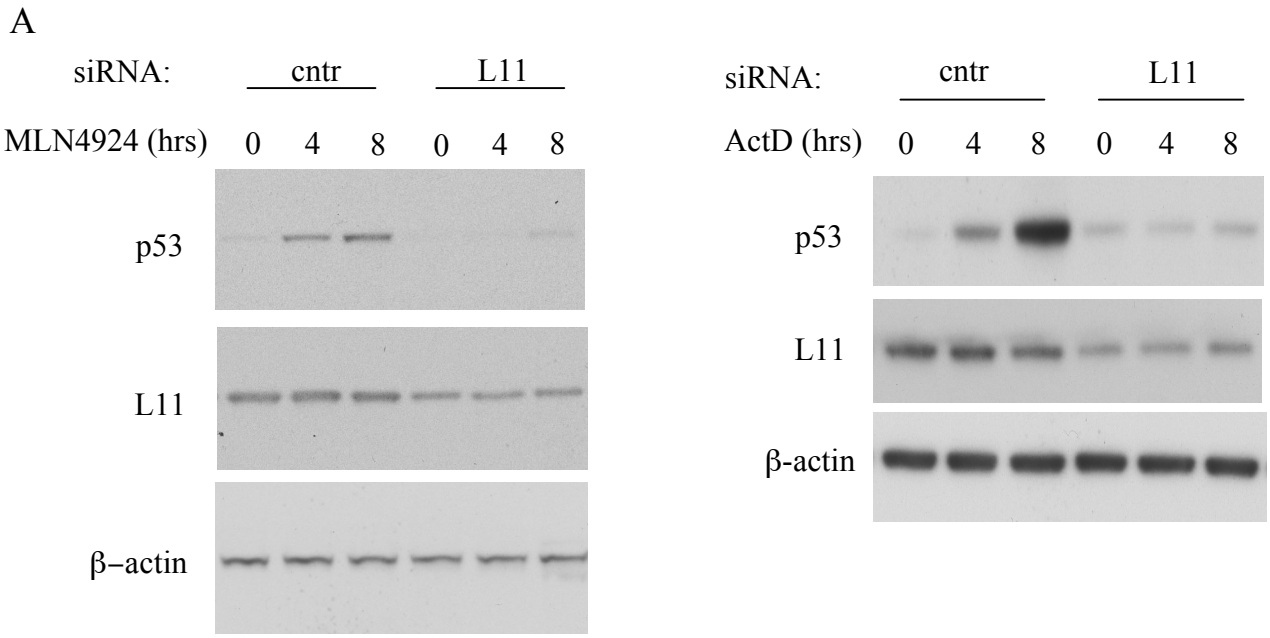
A
siRNA:
cntr
L11
MLN4924 (hrs)
0 4 8 0 4 8
p53
L11
β–actin
siRNA:
cntr
L11
ActD (hrs)
0 4 8 0 4 8
p53
L11
β-actin

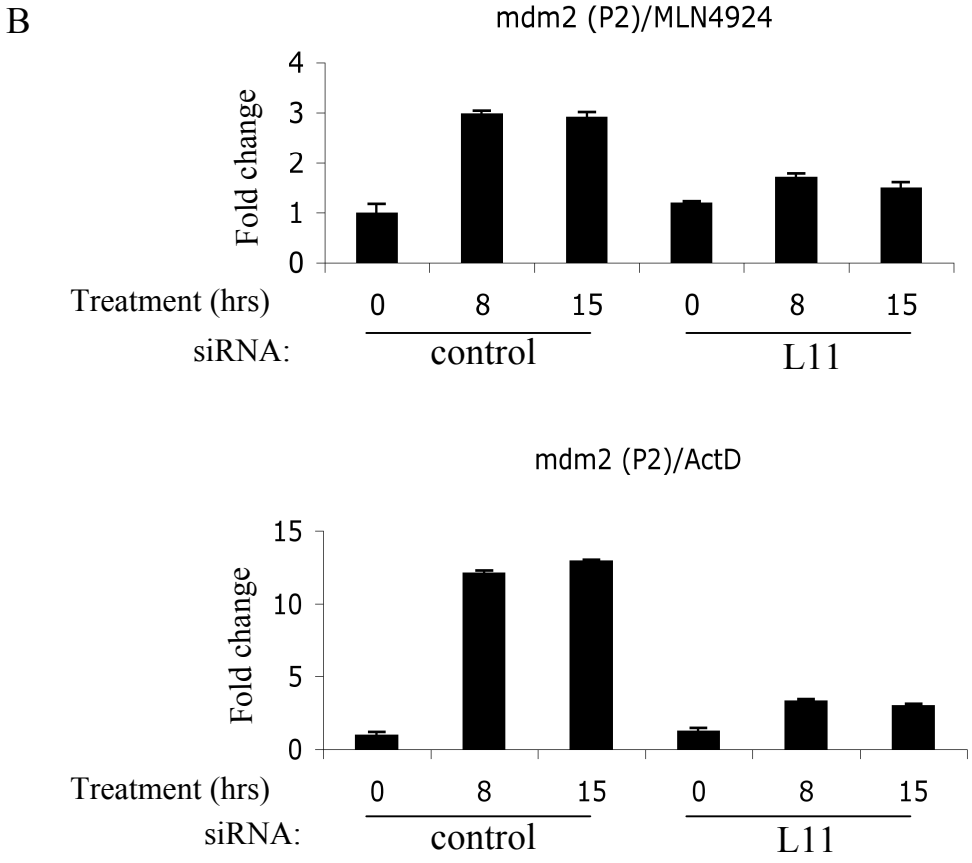
B
mdm2 (P2)/MLN4924
Fold change
4
3
2
1
0
Treatment (hrs)
0 8 15 0 8 15
siRNA:
control
L11
mdm2 (P2)/ActD
Fold change
15
10
5
0
Treatment (hrs)
0 8 15 0 8 15
siRNA:
control
L11

Figure 4

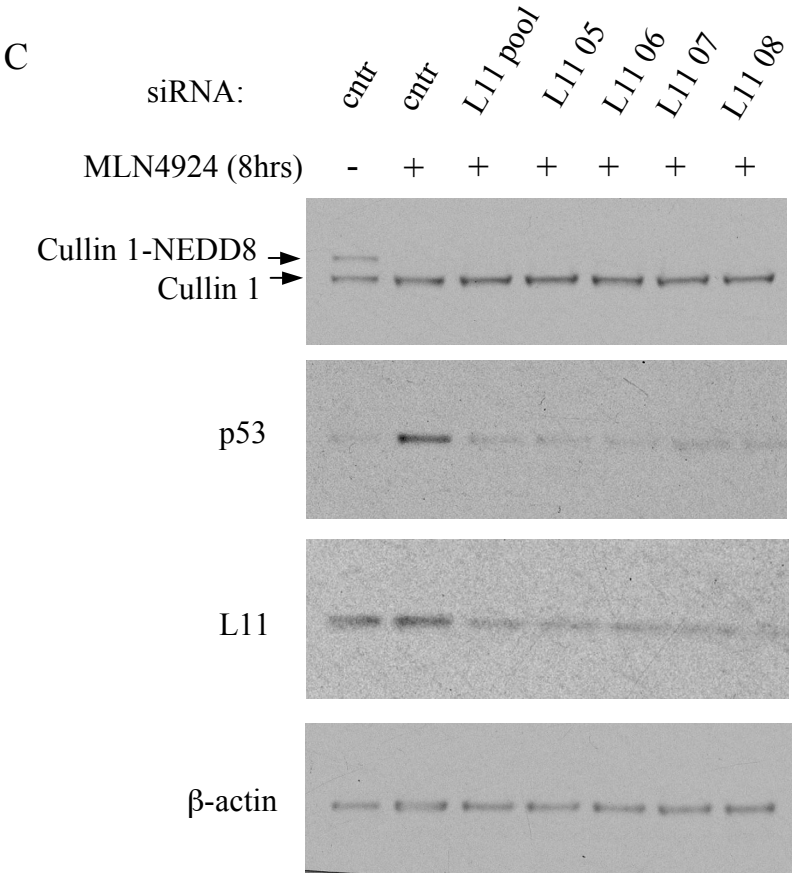
C
siRNA:
cntr
cntr
L11 pool
L11 05
L11 06
L11 07
L11 08
MLN4924 (8hrs)
- + + + + + +
Cullin 1-NEDD8
Cullin 1
p53
L11
β-actin

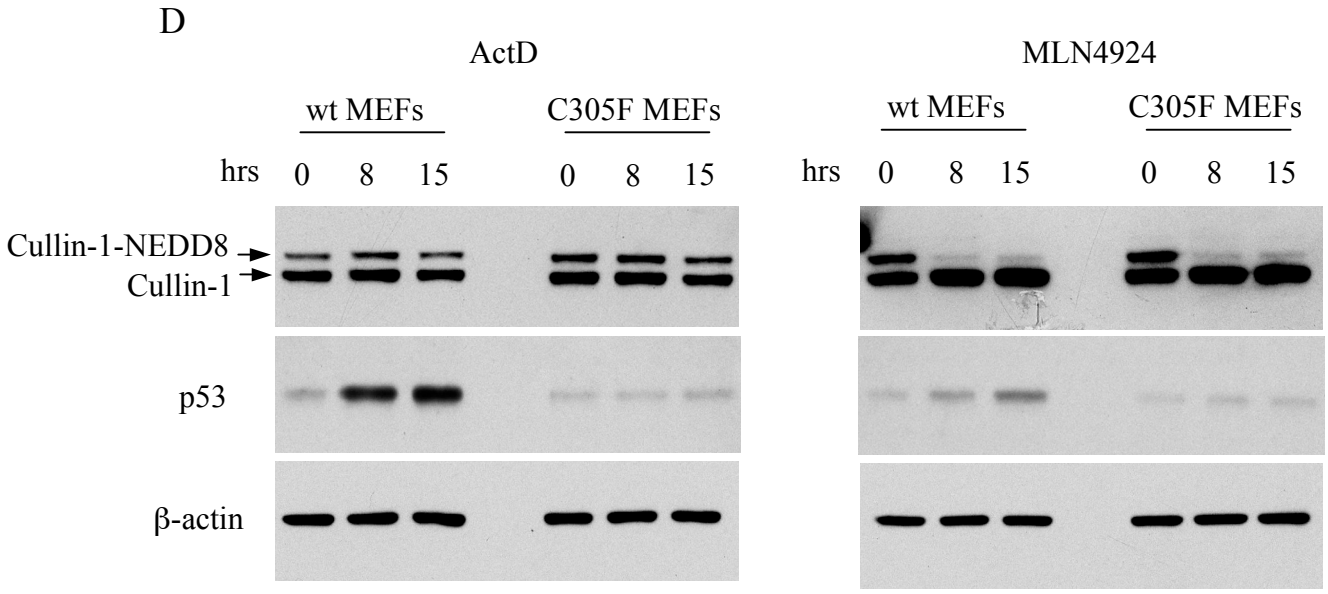
D
ActD
MLN4924
wt MEFs
C305F MEFs
wt MEFs
C305F MEFs
hrs 0 8 15 0 8 15
hrs 0 8 15 0 8 15
Cullin-1-NEDD8
Cullin-1
p53
β-actin

Figure 4

E

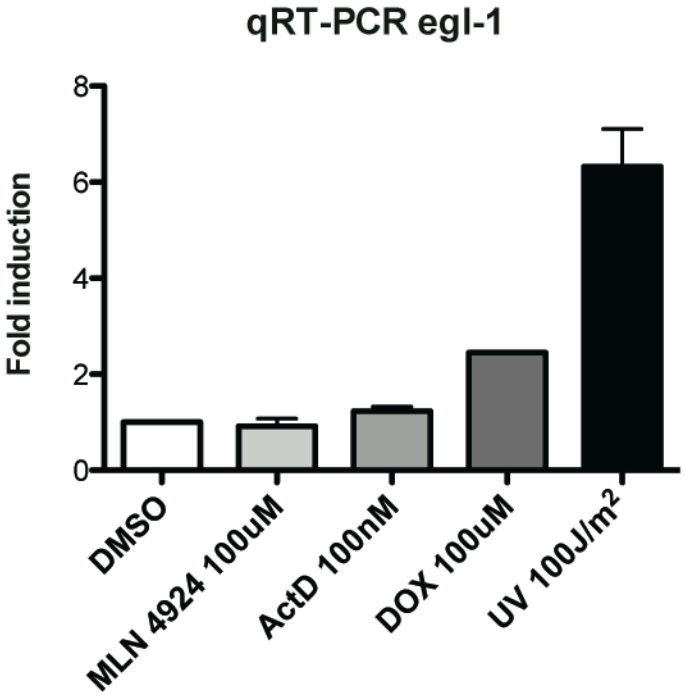
qRT-PCR egl-1
Fold induction
8
6
4
2
0
DMSO
MLN 4924 100uM
ActD 100nM
DOX 100uM
UV 100J/m2

Figure 5

A

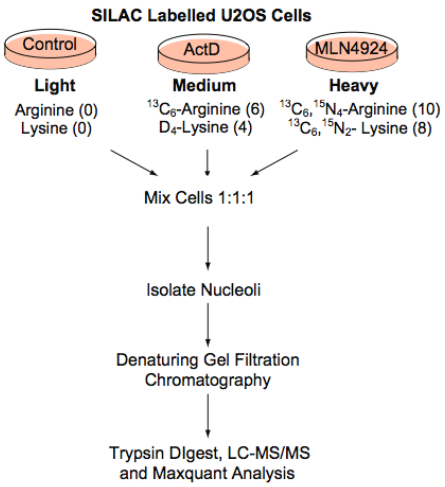
SILAC Labelled U2OS Cells
Control
ActD
MLN4924
Light
Arginine (0)
Lysine (0)
Medium
$^{13}C_6$-Arginine (6)
D_4-Lysine (4)
Heavy
$^{13}C_6$,$^{15}N_4$-Arginine (10)
$^{13}C_6$,$^{15}N_2$- Lysine (8)
Mix Cells 1:1:1
Isolate Nucleoli
Denaturing Gel Filtration Chromatography
Trypsin DIgest, LC-MS/MS and Maxquant Analysis

B

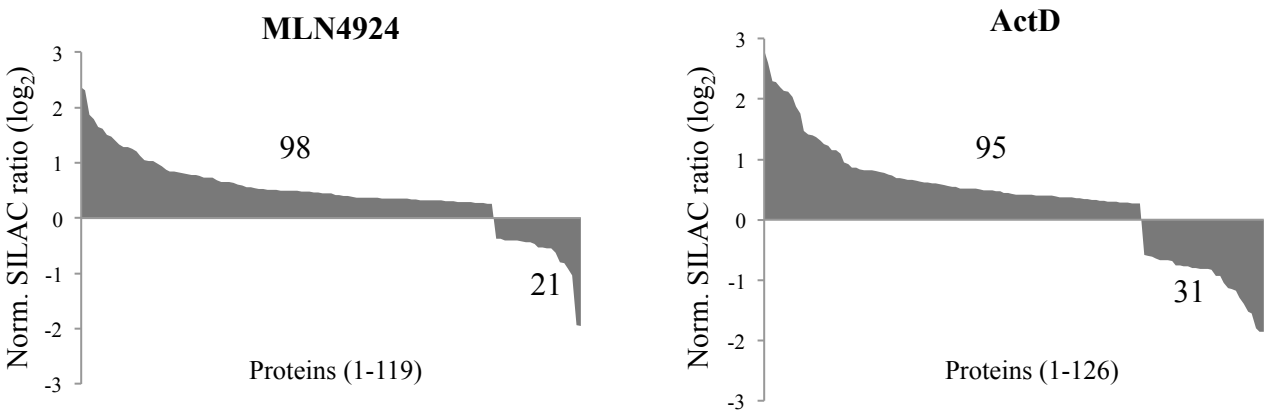
MLN4924
Norm. SILAC ratio (log_2)
3
2
1
0
-1
-2
-3
98
21
Proteins (1-119)
ActD
Norm. SILAC ratio (log_2)
3
2
1
0
-1
-2
-3
95
31
Proteins (1-126)

Figure 5

C

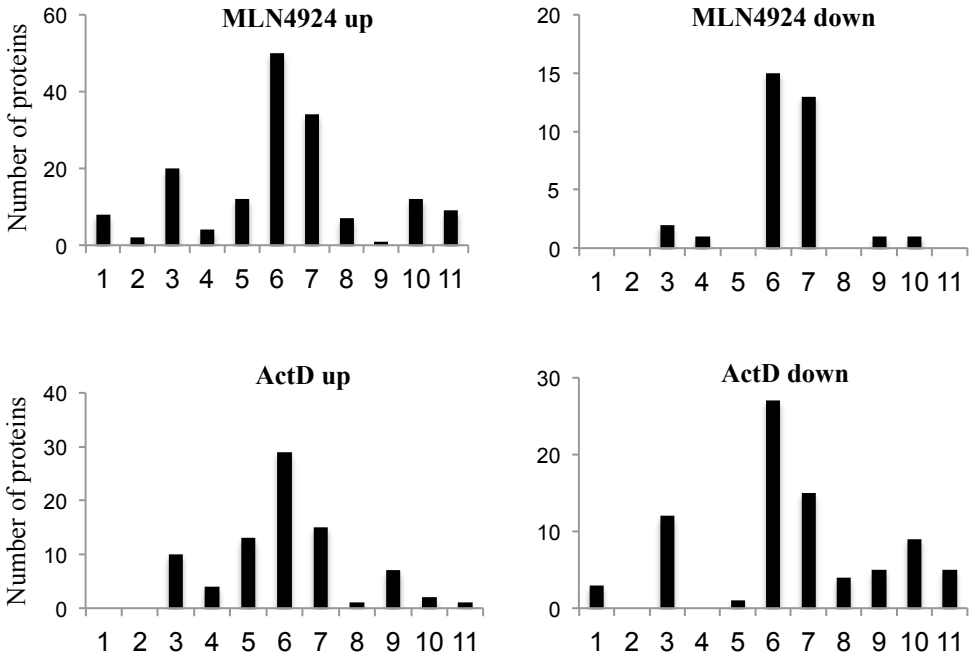

1: apoptosis
2: cell adhesion
3: cell cycle
4: chromosome segregation
5: transport
6: metabolic processes
7: nucleic acid binding
8: transcription factors
9: RNA processing
10: DNA replication
11: DNA repair

D

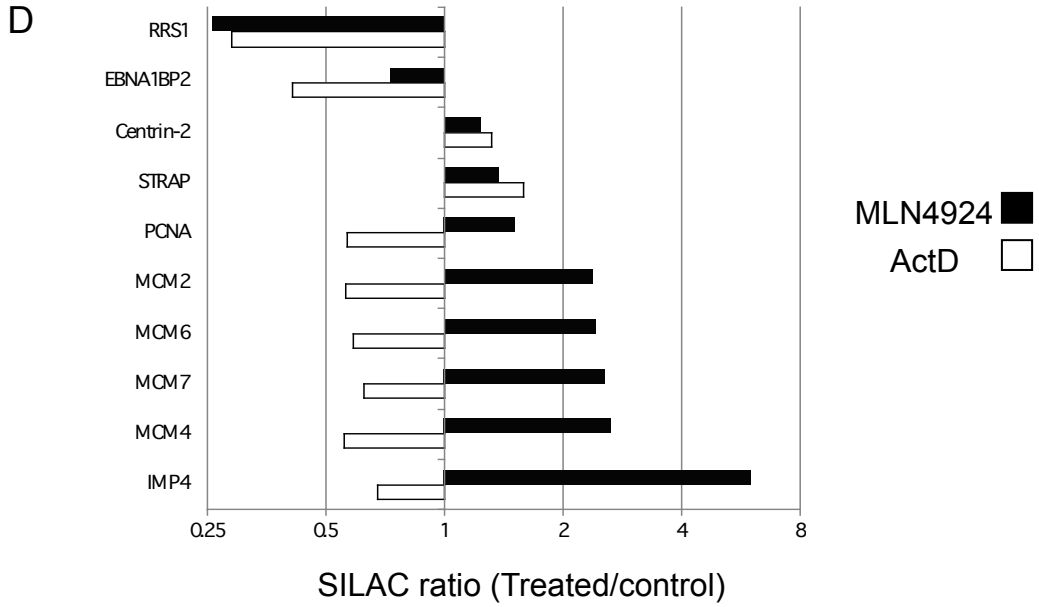

Figure 5

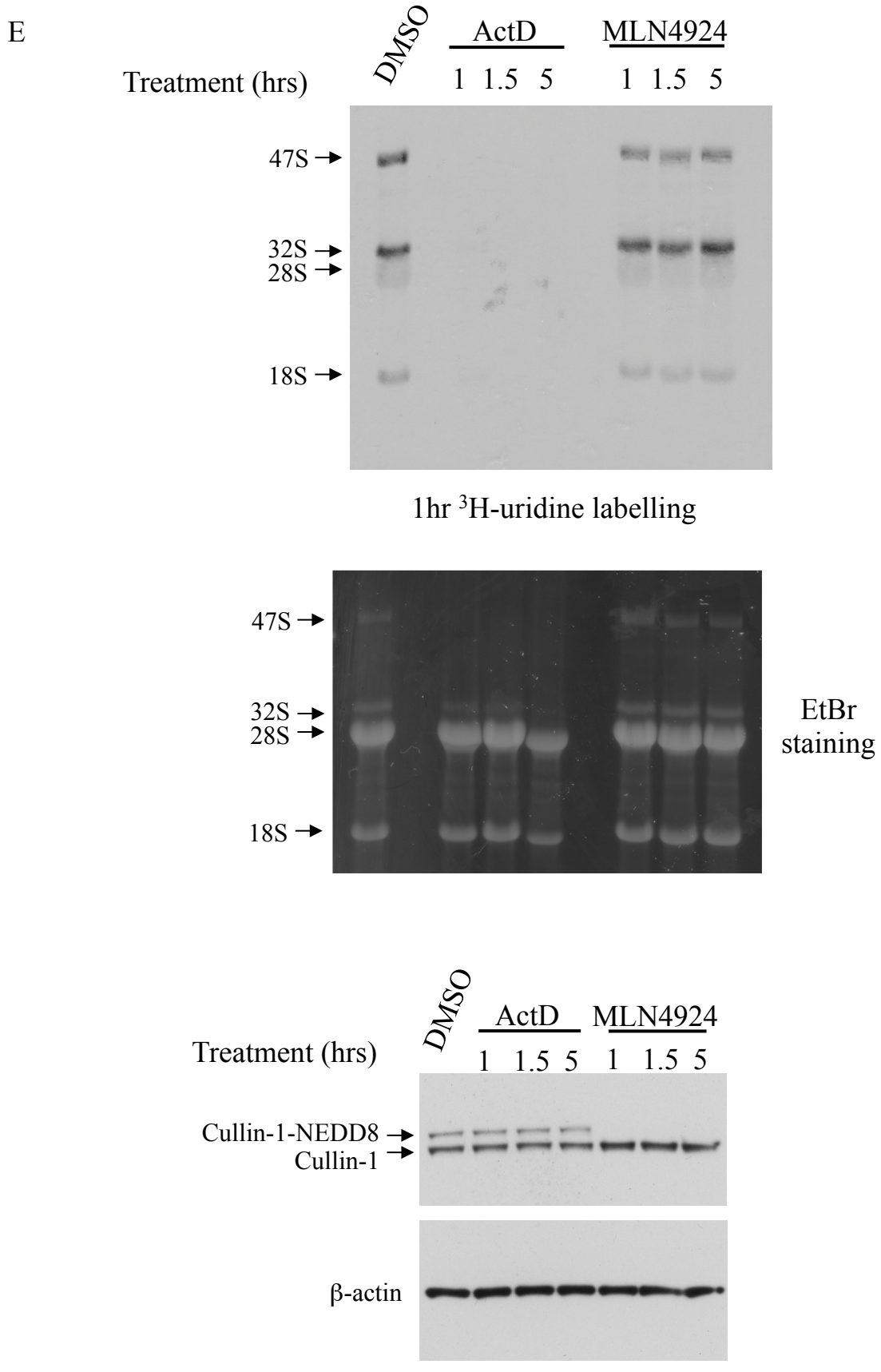
E
DMSO
ActD
MLN4924
Treatment (hrs)
1 1.5 5 1 1.5 5
47S
32S
28S
18S
1hr 3H-uridine labelling
47S
32S
28S
18S
EtBr staining
DMSO
ActD
MLN4924
Treatment (hrs)
1 1.5 5 1 1.5 5
Cullin-1-NEDD8
Cullin-1
β-actin

Figure 5

F

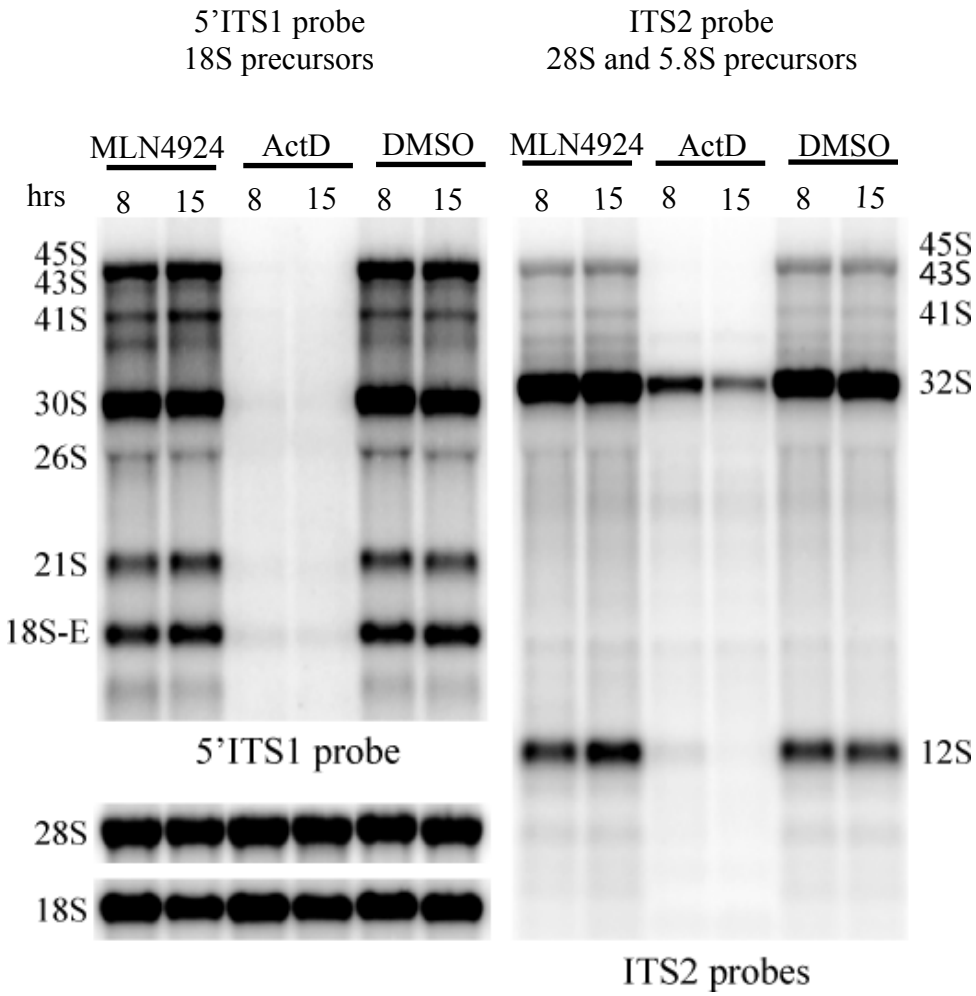
5'ITS1 probe
18S precursors
ITS2 probe
28S and 5.8S precursors
MLN4924
ActD
DMSO
MLN4924
ActD
DMSO
hrs
8
15
8
15
8
15
8
15
8
15
8
15
45S
43S
41S
30S
26S
21S
18S-E
45S
43S
41S
32S
12S
5'ITS1 probe
28S
18S
ITS2 probes

Figure 5

G

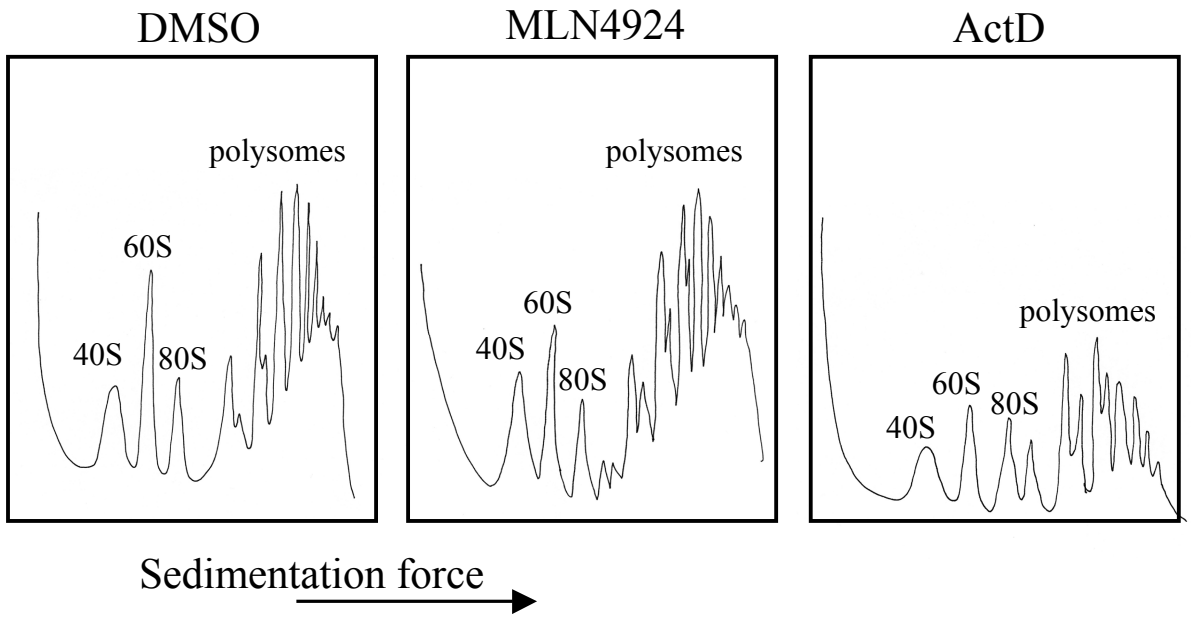
DMSO
MLN4924
ActD
polysomes
60S
40S
80S
polysomes
60S
40S
80S
polysomes
60S
80S
40S
Sedimentation force

Figure 6

A

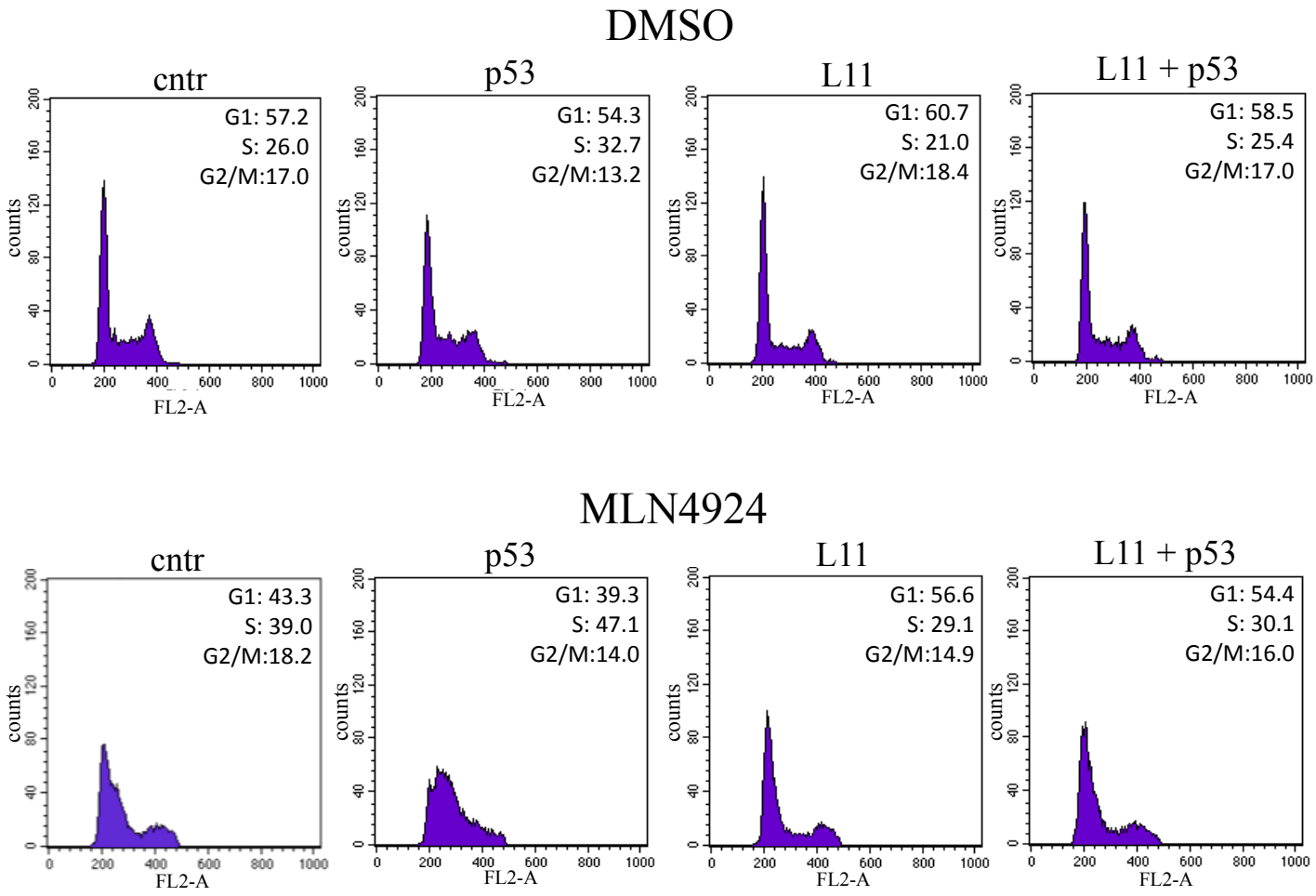
DMSO
cntr
G1: 57.2
S: 26.0
G2/M:17.0
p53
G1: 54.3
S: 32.7
G2/M:13.2
L11
G1: 60.7
S: 21.0
G2/M:18.4
L11 + p53
G1: 58.5
S: 25.4
G2/M:17.0
MLN4924
cntr
G1: 43.3
S: 39.0
G2/M:18.2
p53
G1: 39.3
S: 47.1
G2/M:14.0
L11
G1: 56.6
S: 29.1
G2/M:14.9
L11 + p53
G1: 54.4
S: 30.1
G2/M:16.0
counts
FL2-A

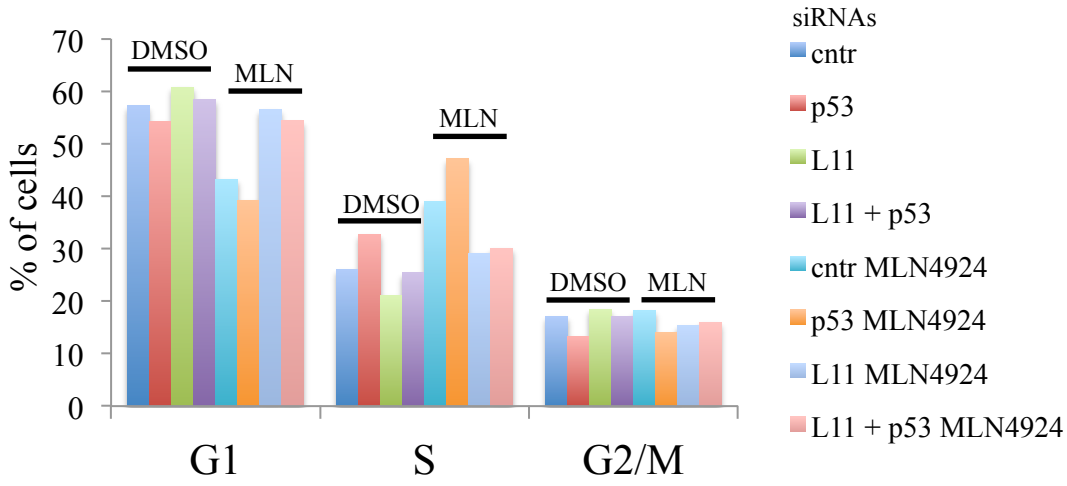
% of cells
DMSO
MLN
G1
S
G2/M
siRNAs
cntr
p53
L11
L11 + p53
cntr MLN4924
p53 MLN4924
L11 MLN4924
L11 + p53 MLN4924

Figure 6

B

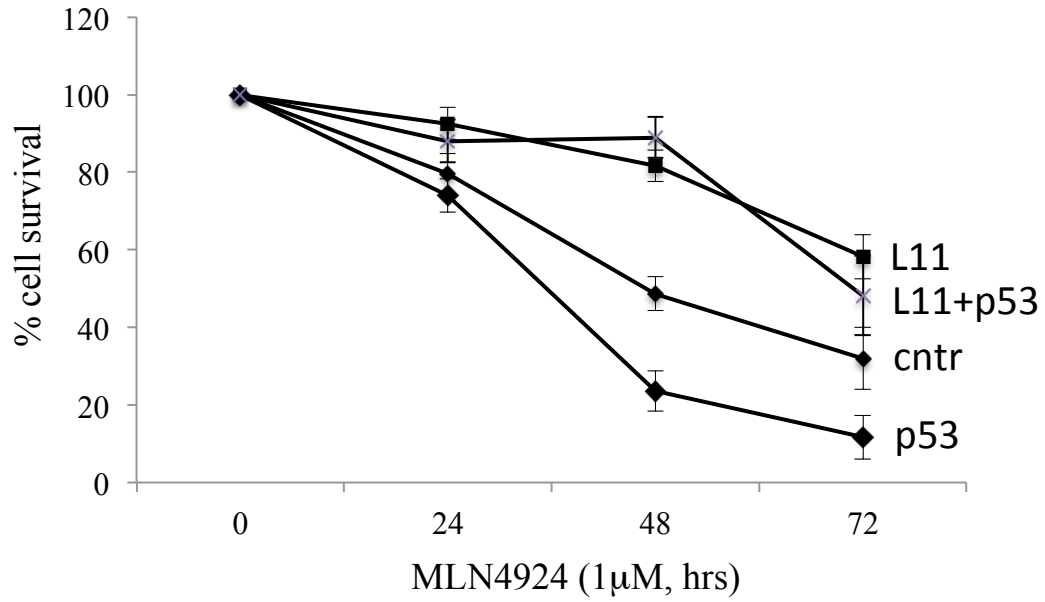
120
100
80
60
40
20
0
% cell survival
0
24
48
72
MLN4924 (1μM, hrs)
L11
L11+p53
cntr
p53

C

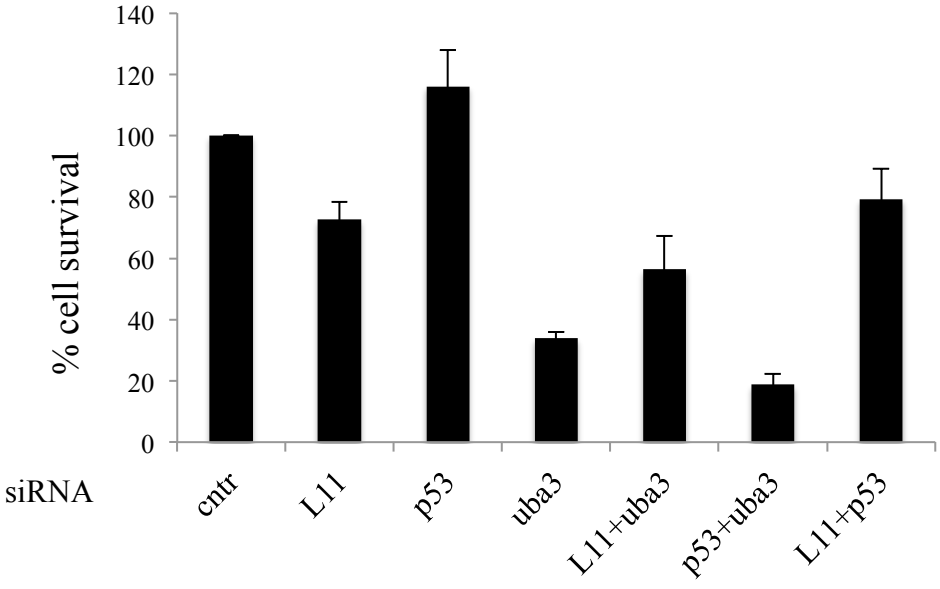
140
120
100
80
60
40
20
0
% cell survival
siRNA
cntr
L11
p53
uba3
L11+uba3
p53+uba3
L11+p53

The NEDD8 inhibitor MLN4924 increases the size of the nucleolus and activates p53 through the ribosomal-Mdm2 pathway

Aymeric Bailly, Aurelien Perrin, Lara Bou Malhab, Emmanuelle Pion, Mark Larance, Manjula Nagala, Peter Smith, Marie-Françoise O'Donohue, Pierre-Emmanuel Gleizes, Joost Zomerdijk, Angus I. Lamond and Dimitris P. Xirodimas

Supplementary information

Materials and Methods

Antibodies and chemicals

DO-1 mouse monoclonal antibody was used for p53 detection, rabbit anti-L11 was a gift from Karen Vousden, mouse anti-β-actin (Oncogene Research Products), mouse anti-Cullin-1 (Zymed), mouse anti-FLAG, mouse anti-aTubulin (Sigma-Aldrich), rabbit anti-Cullin-4A, rabbit anti-nucleolin, rabbit anti-RPL5, mouse anti-fibrillarin mAb (Abcam), rabbit anti-B23 (Sigma), rabbit anti-MCM2, rabbit Calnexin (Cell Signaling), rabbit anti-p21 (Santa Cruz). Actinomycin D, Doxorubicin and G418 were purchased from Sigma-Aldrich, MLN4924 from Active Biochem. The BCA protein assay kit was purchased from Pierce. Triscarboxyethylphosphine (TCEP) (Bond-breaker neutral pH solution) was from Pierce (Rockford, IL). Trypsin was from Promega (Madison, WI). Oasis HLB 96-well m-elution 96-well plates were from Waters (Rockford, CA). The Pepmap C18 columns and trapping cartridges were from Dionex (Sunnyvale, CA). Complete protease inhibitor cocktail tablets and PhosStop phosphatase inhibitor tablets were from Roche (Indianapolis, IN). Lavapep assay reagents were from GelCompany (San Francisco, CA). All other materials were obtained from Sigma-Aldrich (St. Louis, MO). All siRNAs were purchased from Dharmacon as ON-TARGET*plus* pools or individual duplexes. The control siRNA is a non-target pool.

Cell culture and transfections

Cell lines were grown in Dulbecco's modified Eagle's medium except H1299 grown in RPMI, all supplemented with 10% fetal calf serum. Transfections in H1299 cells were performed with calcium phosphate in 10cm dishes. 5nM of siRNAs were transfected in cells seeded in 6-well dishes with lipofectamine RNAiMAX according to manufacturer's instructions. Cells were harvested 36-48hrs post transfections. H1299 cells stably expressing RPL11-EGFP were selected with 0.5mg/ml of G418.

Gene expression

48hrs post transfection with siRNAs, MCF7 cells were treated with ActD or MLN4924. Promega SV Total RNA Isolation system was used to isolate total RNA. cDNA was made using the Invitrogen SuperScript® III First- Strand Synthesis SuperMix for qRT-PCR with 300ng of RNA. The cDNA was diluted with H_2O 20x and 2µl were used in a 12µl reaction. Quantitative real-time PCR was carried out in an ABI 7500 system using ABI PCR master mix according to the manufacture's instructions. Gravid adult worms were collected from the plates and wash three times to remove bacteria with PBS before introduction in Trizol and frozen at -80°C. Total RNA were extract by Trizol/chloroform and follow by RNeasy® Kit (Qiagen) and cDNA synthesis performed on 300ng of RNA with QuantiTech® Reverse Transcription Kit (Qiagen). qRT-PCR reactions were performed in triplicates, and cDNA was diluted in MesaGreen qPCR Master Mix (Eurogentec) with specific primers. The means measured for levels of transcript of interest (egl-1) were normalised with internal level of transcript control (tubulin tbg-1). For data analysis, maximum quantitative point method was applied and induction was calculated with the equation:

Fold Induction= $2^{((^{\Delta Cp(cDNAegl\text{-}1\text{-}cDNAtbg\text{-})}control)-(^{\Delta Cp(cDNAegl\text{-}1\text{-}cDNAtbg\text{-})}treated))}$

Northern blot analysis of pre-rRNA

Control cells or cells treated for 8hrs or 15hrs with ActD or MLN4924 were collected, rinsed with PBS and centrifuged. Total RNAs from 7×10^6 cells were then extracted with Trizol reagent, and further purified with phenol/chloroform/isoamyl alcohol (25:24:1) and chloroform extractions. After alcohol precipitation of the aqueous phase and extensive washings with 70% ethanol, RNA pellets were dissolved in formamid, denatured at 70°C for 10 min, and quantified using a Nanodrop spectrophotometer (Thermo Fisher Scientific). Pre-RNAs (3µg total RNAs/well) were separated on a 1.1% agarose gel prepared with Tri/Tri buffer (30mM tri-ethanolamine, 30mM tricine, pH 7.9) containing 1.2% formaldehyde, and run in Tri/Tri buffer at 140 volts. RNAs were then transferred to a Hybond N^+ nylon membrane (GE Healthcare, Orsay, France) and fixed by UV-cross-linking. The membrane was pre-hybridized for 1hr at 45°C (6× SSC, 5× Denhardt's solution, 0.5% SDS, 0.9µg/ml tRNA). The ^{32}P-labelled oligodeoxynucleotide probe was then incubated overnight at 45°C. The probes used were: 5'ITS1 (5'-cctcgccctccgggctccgttaatgatc-3'), that reveals all the 18S precursors; a mixture of ITS2b (5'-ctgcgagggaacccccagccgcgca-3') and ITS2d/e (5'-gcgcgacggcggacgacaccgcggcgtc-3'), that reveal 5.8S and 28S precursors; 18S (5'-tttacttcctctagatagtcaagttcgacc-3'); 28S (5'-cccgttcccttggctgtggtttcgctagata-3'). After hybridization, the membrane was washed twice for 10min at room temperature in 2× SSC, SDS 0.1%, and once in 1× SSC, SDS 0.1%. Labelled RNA signals were acquired with a Typhoon Trio Imager (GE Healthcare) and quantified with the ImageGauge software.

RNAi bacterial growth conditions (*C. elegans*)

E. coli HT115 RNAi bacteria were grown in M9 minimal medium, prepared by mixing 100ml of 10x M9 salts (420mM disodium phosphate, 240 mM monopotassium phosphate, 90mM sodium chloride, 190mM ammonium chloride) and deionized water and autoclaved (120 °C for 20 min). 1ml of M9 bacterial 1X is completed by 5µl of 40% (wt/vol) glucose, 1µl of 1M $MgSO_4$, 1µl of 1% (wt/vol) thiamine and 1µl of 100mg/ml ampicillin. A single bacteria colony streaked on LB plate is used to start the culture at 37°C under agitation until OD600=1. Bacteria culture is seeded on NGM plates. Worms are placed on NGM plates seeded with RNAi bacteria at late L4 stage during 24 hours and dissected.

Nucleoli size quantification with Image J software

Images were imported into Image J (http://rsb.info.nih.gov/ij/) as tiff files. (A, B) The first step was to adjust the minimal fluorescence threshold representative for DAPI and FIB-1 staining to define the perimeter of nucleus and nucleolus to exclude background and determine the area. (Command "Image>Adjust>Threshold") (C, D). The free hand tool was used and a circle was drawn around the nuclei to measure (Command "Measure") the number of pixels included between the minimal and maximal threshold analysed by software. In the circle only the higher level of intensity established by the minimal threshold was included in the measurement, which is independent of labelling intensity. Measurements were analysed by excel to compare the size of the nucleus and the nucleolus. The relative size of the nucleolus was determined by dividing the nucleolar/nuclear intensity and presented as % change.

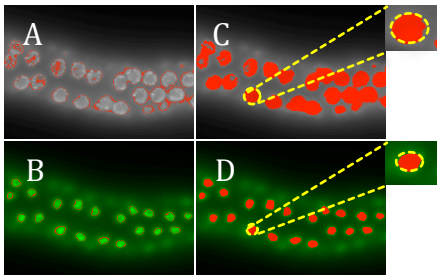

	DAPI			**FIB-1**		
	Area (Pixels)	**Minimum intensity include**	**Maximum intensity**	**Area (Pixels)**	**Minimum intensity include**	**Maximum intensity**
DMSO_	**2013**	1501	2159	**523**	1925	2598

Detection of newly synthesised RNA

Transcription efficiency was monitored by ^{3}H-uridine incorporation of newly synthesized RNAs as previously described [1]. H1299 cells were seeded in 6 well plates and were either DMSO, ActD or MLN4924 treated. Cells were pulsed with 3μCi/ml of ^{3}H-uridine for 1 hr at 37^{o}C. Cells were washed once with PBS and total RNA was isolated using RNAeasy kit (Qiagen) following manufacturer's instructions. 4mg of RNA was subjected to agarose-formaldehyde gel electrophoresis. The EtBr-stained gel was photographed and electroblotted onto GE Nylon, Positively Charged Transfer Membrane. The ^{3}H-labeled RNA was UV-irradiated, sprayed with tritium enhancer (Perkin Elmer) and exposed to Kodak X-ray film for 3 days.

Staining

Worms were dissected on poly lysine coated slides in PBS. Germlines were then fixed in 1.8% formaldehyde for 5 min at room temperature followed by freeze cracking in liquid nitrogen. Post-fixation was done in a 1:1 mixture of methanol:acetone at −20°C, followed by permeabilization with PBS+ 1% Triton X-100 (three times for 10 min, room temperature). Samples were blocked with Image-iT FX signal enhancer (Invitrogen) for 20 min, followed by 15 min of incubation in PBS+ 0.1% Tween 20+1%BSA (PBSTB). Primary antibodies were diluted in PBSTB at 4°C overnight in a humid chamber. Samples were washed three times for 10 min in PBS + 0.1% Tween 20 (PBST). Secondary antibodies were incubated for 2h at room temperature diluted in PBSTB supplemented with 1μg/μl DAPI. After washing three times for 10 min in PBST, the samples were mounted in Vectashield mounting medium (Vector laboratories). Pictures were acquired with a Zeiss Axioimager Z2 using metamorph software. Anti-fibrillarin antibody was used at 500x dilution and the secondary Alexa goat-anti-mouse 488, combined with DAPI at 500x dilution.

Fluorescence Recovery After Photobleaching (FRAP)

H1299 cells stably expressing RPL11-EGFP were seeded in glass-bottom dishes (WILCO, Intracel) and treated with ActD and MLN4924 for 4hrs as indicated. Cells were placed in a temperature-controlled chamber at 37 C (Solent Scientific, UK). Nucleoli were photobleached for 0.1 sec with a 488 nm, 20 mW laser at 10% power focussed through a 60x oil immersion objective. This provided approximately 60% decrease in EGFP signal. Data were acquired from 20 randomly selected nucleoli. For each nucleolus, 32 images were captured within 15 sec and data were analysed with SoftWorx (Applied Precision, Seattle).

Subcellular fractionation and proteomics

Denaturing Gel Filtration Chromatography, Trypsin Digestion and Peptide Clean-up

Using a Dionex Ultimate 3000 HPLC system, subcellular fractions in 6M guanidine-HCl were injected (20µl per injection – 40µg protein) onto a mAbPacSEC column from Dionex equilibrated with 6M Urea, 2M Thiourea, 0.1M Tris-HCl pH 7.0 flowing at a rate of 0.2ml per minute and collecting 32x50 µl fractions in a deep-well low protein binding 96-well plate (Eppendorf). Three volumes of 0.1M Tris-HCl pH 8.0, 1mM $CaCl_2$ was added to each fraction to dilute the urea, trypsin was subsequently added at a ratio of 1:50. The plate was sealed with a rubber mat, vortexed and incubated overnight at 37^{o}C. Trifluoroacetic acid was added to 1% final concentration and peptides purified using an Oasis HLB 96-well m-elution 96-well plate. Peptides were eluted in 100µl of acetonitrile and speedivaced to dryness prior to resuspension in 5% formic acid. Peptide concentration was determined using a Lavapep assay after 500-fold dilution of peptide samples.

LC-MS/MS and Maxquant Analysis

Using a Dionex Ultimate 3000 nanoHPLC system, 1μg of peptides in 5% formic acid were injected onto an Acclaim PepMap C18 nano-trap column (Dionex). After washing with 2% acetonitrile 0.1% formic acid peptides were resolved on a 150mm x 75μm Acclaim PepMap C18 reverse phase analytical column over a 100min organic gradient with a flow rate of 250nL/min. Peptides were ionised by nano-electrospray ionisation at 1.2kV using a stainless steel emitter with an internal diameter of 0.005 mm (Proxeon, Denmark). Tandem mass spectrometry analysis was carried out on a LTQ-Velos Orbitrap mass spectrometer Thermo Scientific (San Jose, CA).

The data dependent acquisition method used was the FT10 protocol as described previously [2]. Data were processed, searched and quantified using the Maxquant software version 1.1.1.14 package as described previously [3] using the default settings using the human Swissprot and Tremble database version. The settings used for the Maxquant analysis were: 2 missed cleavages allowed; enzyme was Trypsin cleaving after arginine and lysine; variable modifications were methionine oxidation; deamidation of glutamine or asparagine; peptide N-terminal pyro-glutamic acid; protein N-terminal acetylation; a mass tolerance of 7ppm was used for precursor ions and a tolerance of 0.5Da was used for fragment ions. Using the default Maxquant settings a maximum false positive rate of 1% is allowed for both peptide and protein identification this is used as a cut-off score for accepting individual spectra as well as whole proteins in the combined search and quantitation output. This threshold has previously been shown to be a rigorous method of identifying true positive matches [3]. Protein quantitation data was always derived from two or more peptides per protein.

References

1. Pestov DG, Lapik YR, Lau LF. Assays for ribosomal RNA processing and ribosome assembly. *Curr Protoc Cell Biol* 2008; **Chapter 22**, Unit 22, 11.
2. Haas W. *et al.* Optimization and use of peptide mass measurement accuracy in shotgun proteomics. *Mol Cell Proteomics* 2006; **5**: 1326-1337.
3. Cox J, Mann, M. MaxQuant enables high peptide identification rates, individualized p.p.b.-range mass accuracies and proteome-wide protein quantification. *Nat Biotechnol* 2008; **26**: 1367-1372.
4. Brangwynne CP, Mitchison TJ, Hyman AA. Active liquid-like behavior of nucleoli determines their size and shape in Xenopus laevis oocytes. *Proc Natl Acad Sci U S A* 2011; **108**:4334-9.

S1

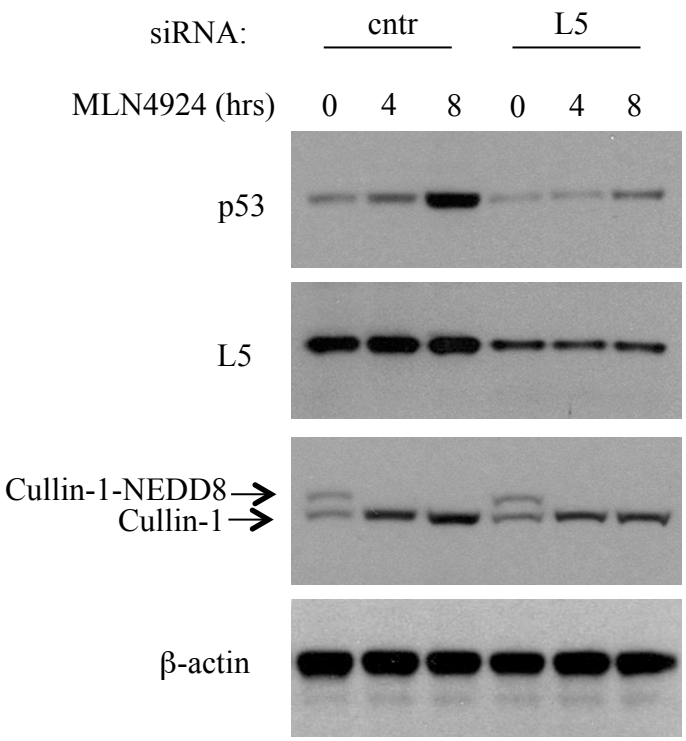

RPL5 is required for p53 stabilisation by MLN4924
MCF7 cells were transfected with either control or RPL5 siRNA before they were treated with MLN4924 as indicated. Total cell extracts were analysed by western blotting.

S2

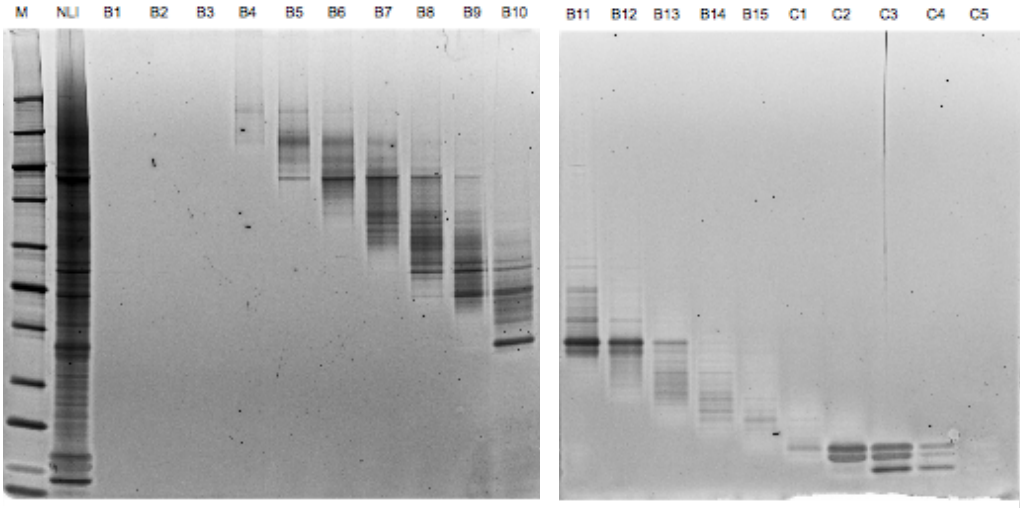

SYPRO Ruby Stain (10µl of 400µl Fractions) of fractions after isolation of nucleoli and denaturing gel filtration (see experimental procedures)

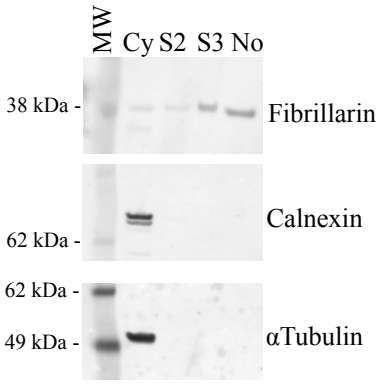

Western blot analysis of different fractions during nucleoli isolation.
Cy: Cytoplasm, S2 and S3: nuclear fractions, No:Nucleoli

S3

MLN4924

A

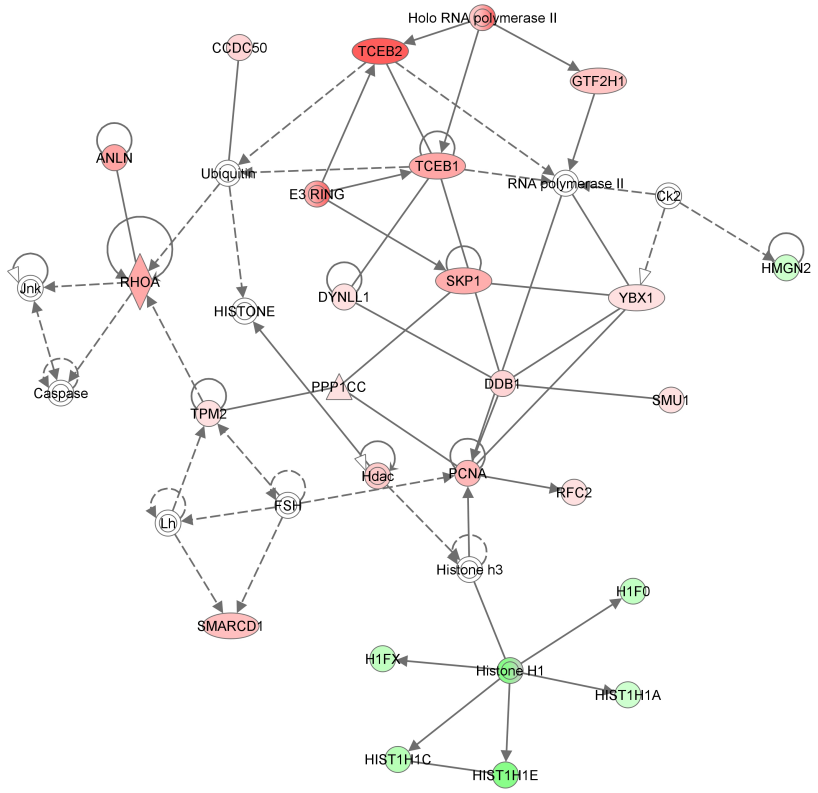

B

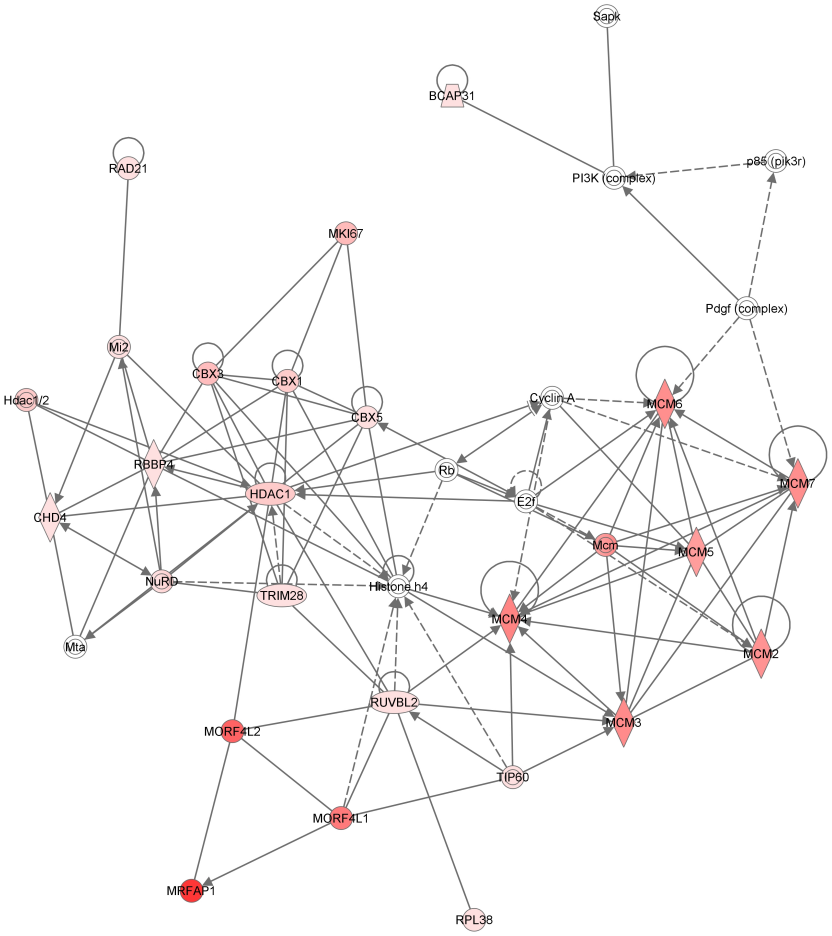

S3

C

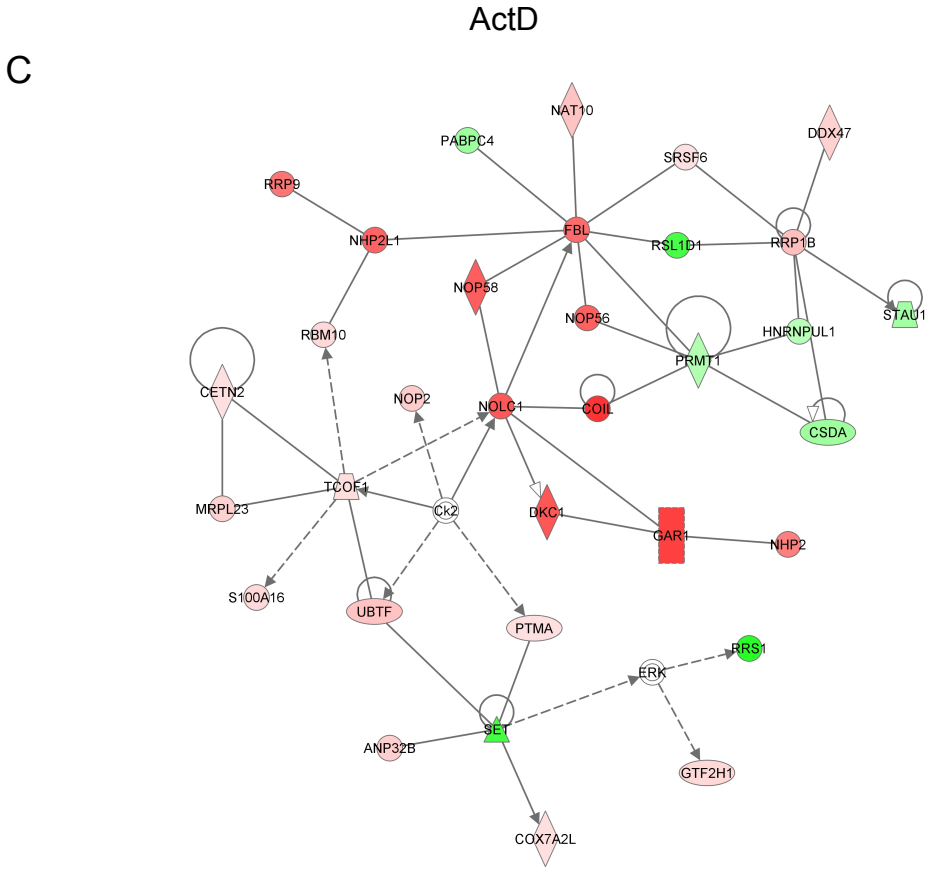

'Ingenuity pathways analysis' (www.ingenuity.com) was used to create networks for proteins affected by MLN4924 (A, B) and ActD (C, next page). The colour indicates the effect of each treatment on the nucleolar abundance for each protein (red: increase, green: decrease). The networks with the highest scores are presented.

S4

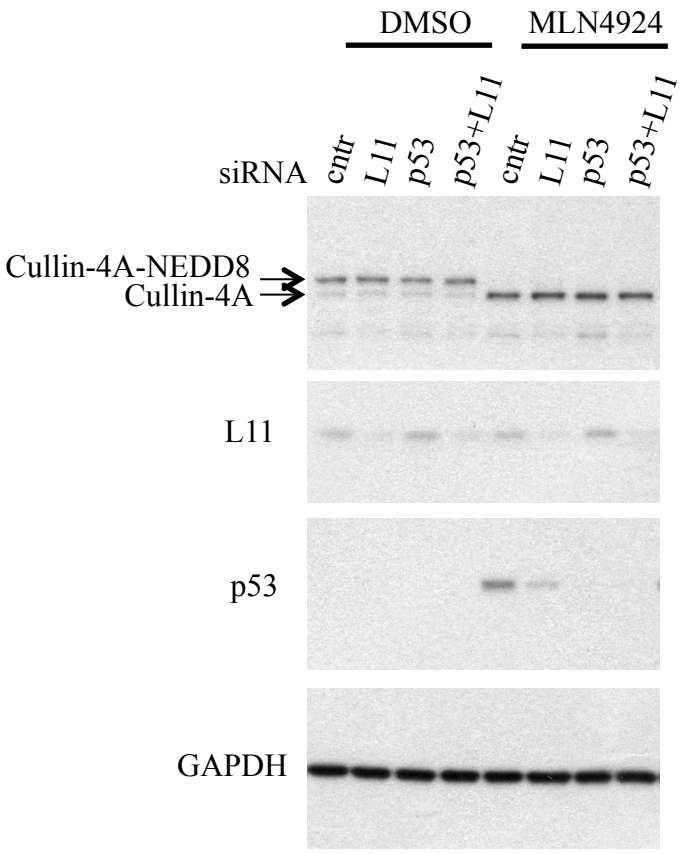

Western blot analysis of cell extracts prepared in 2xSDS buffer from the experiment used for FACS analysis in Fig. 6

S5

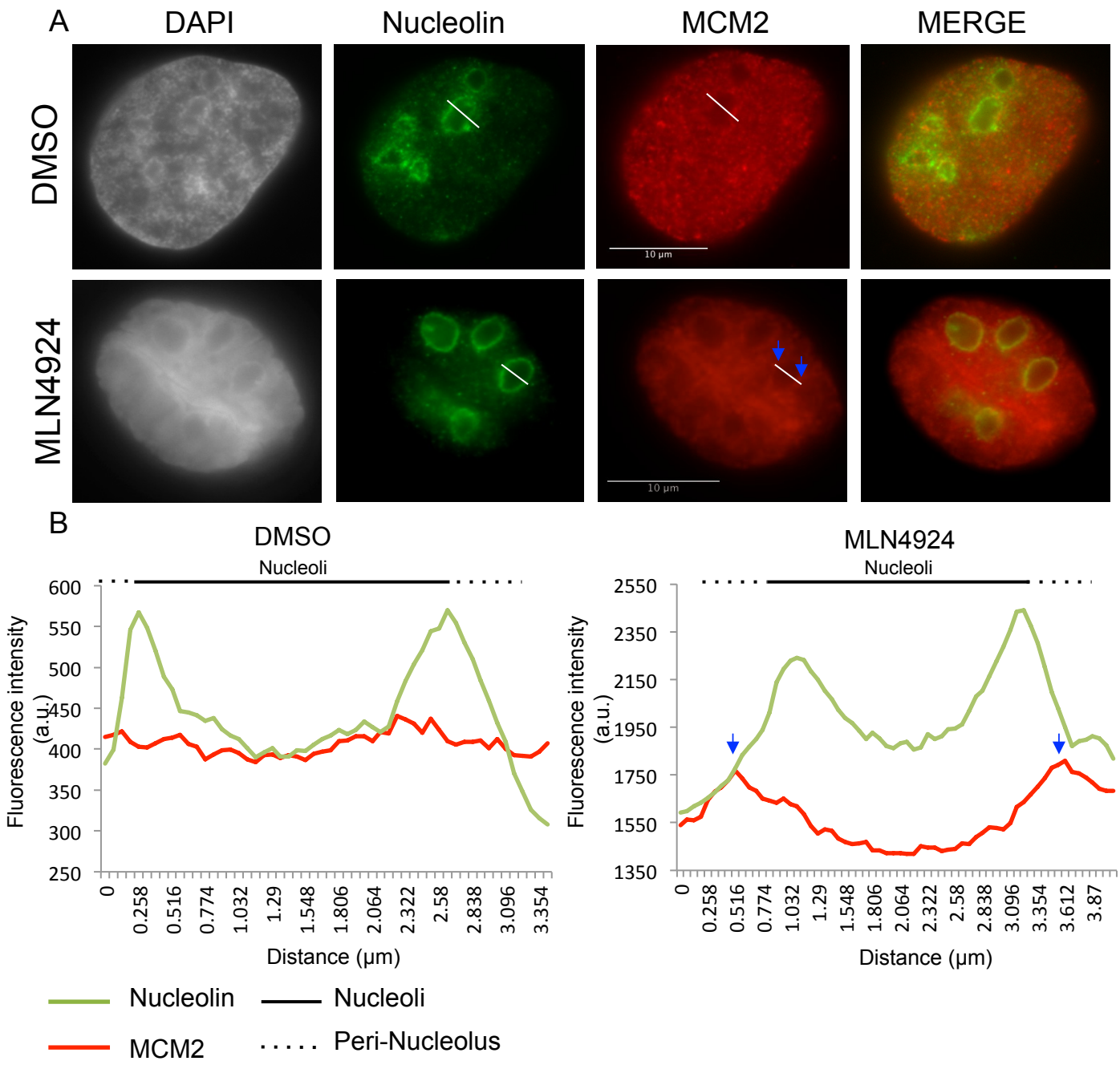

Peri-nucleolar relocalisation of MCM2 upon MLN4924 treatment

(A) U2OS cells were treated with either DMSO or with MLN4924 (1µM) for 24h before cells were fixed and stained for MCM2, Nucleolin and DAPI. (B) Nucleolin staining was used to define nucleoli and fluorescence intensity for nucleolin and MCM2 was measured across the drawn line indicated in A. To quantify the localisation of MCM2 around the nucleoli after MLN4924 treatment, the acquired images were analysed using the Image J software (http://rsb.info.nih.gov/ij/) as described in [4]. For each channel (staining) the plot profile was determined (Command "Analyse>Plot profile") and measurements were exported to excel to make the "Plot profile" graph. The two arrows (blue) show the peri-nucleolar relocalisation of MCM2 after MLN4924 treatment.

S6

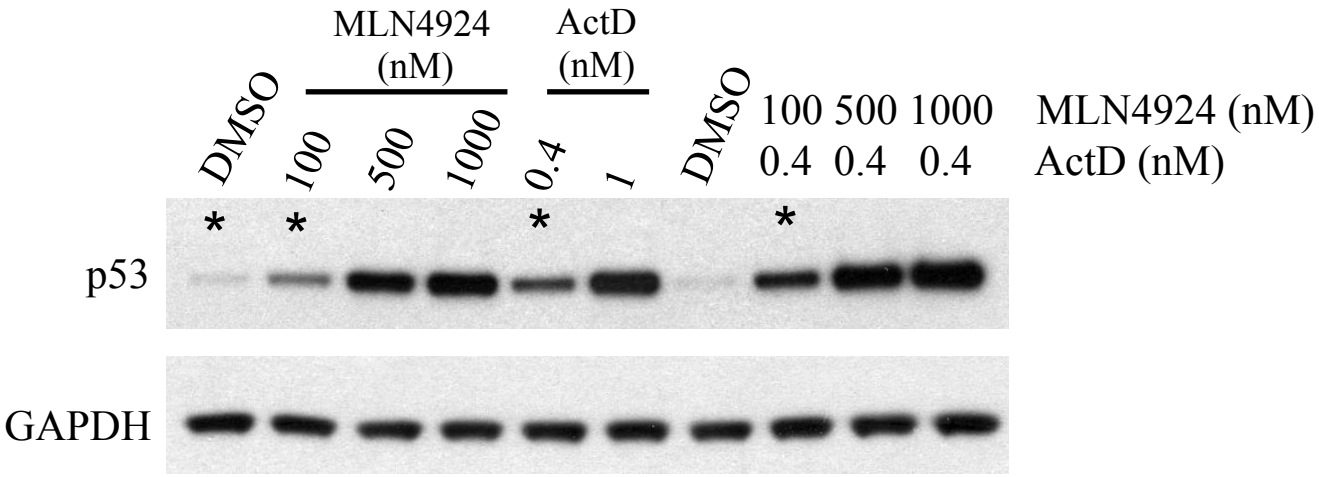

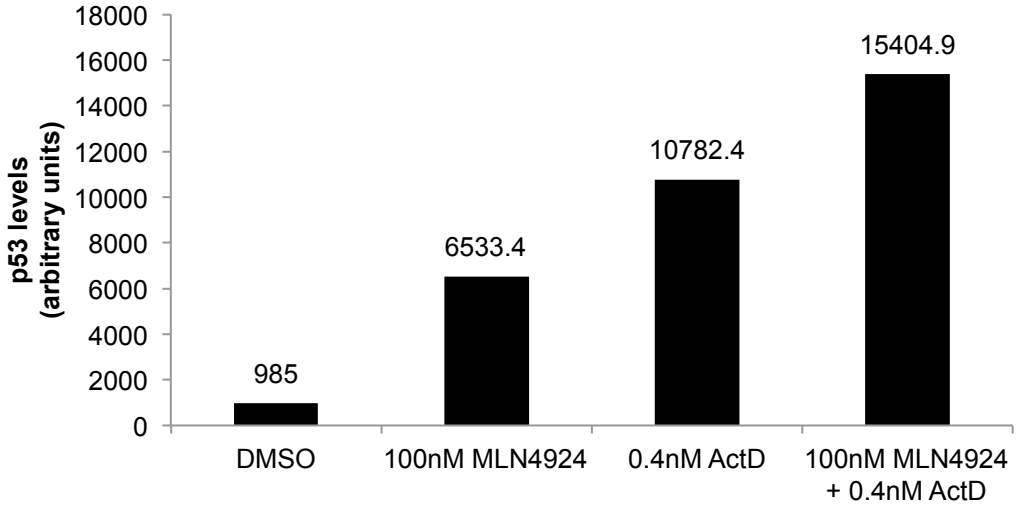

Combination of MLN4924 with ActD produces an additive effect on p53 stabilisation
MCF7 cells were treated with the indicated doses of MLN4924, ActD or with DMSO for 15 hrs. Cells were lysed in 2xSDS and extracts were analysed by western blotting (top panel). The asterisks indicate the bands used for p53 quantitation (lower panel) with Image J.

Nucleolar Isolation Protocol

We recommend that you first download and read this page as a PDF file. Using that as your guide, you can then follow the protocol below and view a Quicktime movie demonstrating the key steps. We have also included higher resolution stills which provide close-ups of certain steps of the protocol.

Special Feature: Complete nucleolar isolation protocol in one Quicktime movie	
Click here to view at high resolution (25.8 Mb) *Warning: this can take a long time to load, depending on the speed of your connection. Please be patient!*	Click here to view at low resolution (9.2 Mb) *This movie loads more quickly than the high resolution version, but some details are difficult to resolve.*
The movie stars Dr. Yun Wah Lam, who optimized the original protocol.	

Buffers and solutions

(All solutions are supplemented with Complete Protease inhibitor tablet (Roche, Cat no: 1-873-580) at the final concentration of 1 tablet/50ml):

PBS
Buffer A: 10 mM Hepes, pH 7.9, 10mM KCl, 1.5mM MgCl2, 0.5mM DTT
S1 solution: 0.25 M Sucrose, 10 mM MgCl2
S2 solution: 0.35 M Sucrose, 0.5 mM MgCl2
S3 solution: 0.88 M Sucrose, 0.5 mM MgCl2

See "Notes" below on making stock sucrose solution.

Procedure

Note: Nucleoli were prepared from HeLa cells using a variation on a method described by Muramatsu and co-workers in 1963 *(Muramatsu M, Smetana, K., and Busch, H.: Quantitative aspects of isolation of nucleoli of the Walker carcinosarcoma and liver of the rat. Cancer Res. 1963; 25:693-697).*

1. Seed HeLa cells (ATCC number: CCL-2) on to 10x14 cm Petri dishes and culture at 37oC in 5% CO2 in Dulbecco's Modified Eagle Medium (DMEM) containing 4mM L-glutamate, 4.5 mg/ml glucose and 0.11 mg/ml sodium pyruvate (Invitrogen UK, Cat no: 41966-029), supplemented with 100 U/ml Penicilin and 100 µg/ml Streptomycin (1% v/v Penicilin/Streptomycin solution, Invitrogen UK, Cat no: 15140-122) until >90% confluence (approx. 107 cells per dish). This number of HeLa cells consistently provides nucleoli with excellent yield and purity. It is possible to scale down the preparation, although purity of the isolated nucleoli may suffer. Make sure you monitor every step using a phase contrast microscope (see below). 1 hour before nucleolar isolation, replace with fresh, pre-warmed medium.

2. Harvest cells by trpysinization. Rinse each dish 3X with pre-warmed PBS, and on removal of the last rinse, add 2 ml of trypsin-EDTA solution (Invitrogen UK, Cat no: 25300-054) per dish. Swirl the dishes to make sure the trypsin-EDTA is evenly distributed, and return the dishes to the incubator for about 5 min. Check under a phase contrast microscope that all the cells are detached. Prolong incubation if needed. Add into each dish 8 ml of pre-warmed medium, pipette up and down so that all the cells are collected as a single-cell suspension. Pool all the harvested cells into 2x 50ml Falcon tubes. For some strains of HeLa cells, it is also possible to

harvest the cells by scraping them in 5 ml ice-cooled PBS per dish. Since scraping may lead to impure nucleolar preparation in some HeLa strains, it is not recommended as the method of first choice.

3. Wash 3 X with ice-cold PBS at 218 g (1000 rpm, Beckman GS-6 centrifuge, GH-3.8 rotor) at 4oC.

4. After the final PBS wash, resuspend the cells in 5ml of Buffer A and incubate the cells on ice for 5 min. Put a small drop of the cell suspension on a glass slide and check under a phase contrast microscope, such as a Zeiss Axiovert 25, using a 20X objective. The cells should be swollen, but not burst (Fig 1). Nucleoli of cultured mammalian cells disassemble at 37oC in hypotonic conditions (Zatsepina et al, 1997). It is therefore imperative to keep the cell suspension on ice during this step.

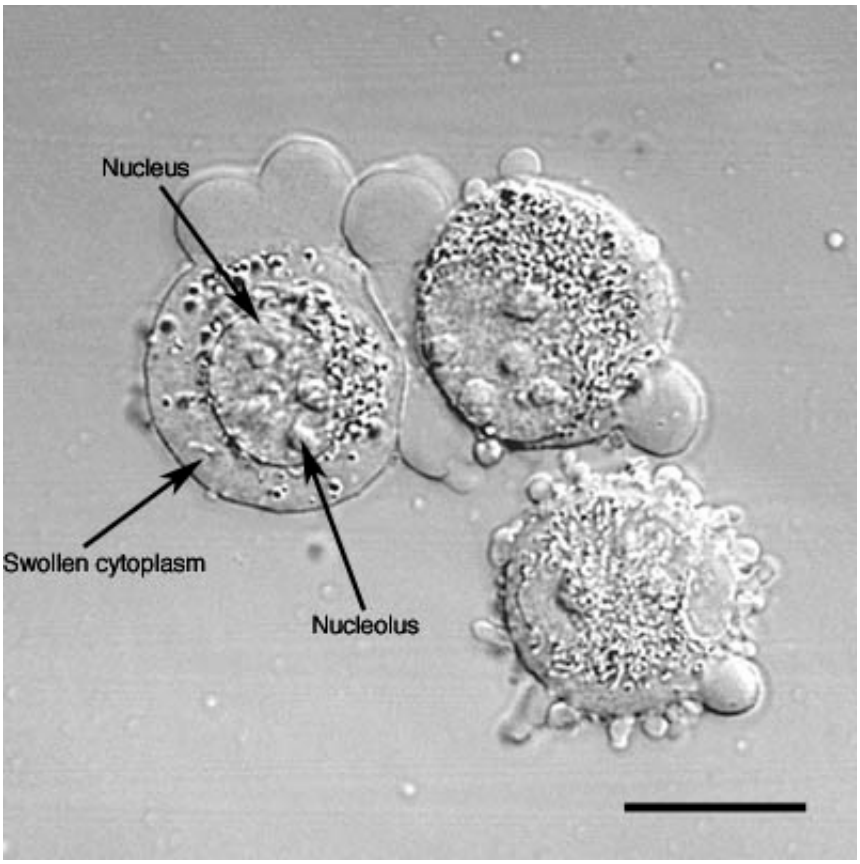

Figure 1: HeLa cells after step 4. Note the swollen cytoplasm and prominent nucleoli. Bar: 10μm.

5. Transfer the cell suspension to a pre-cooled 7 ml Dounce tissue homogenizer (Wheaton Scientific Product Cat no: 357542). Homogenize 10 times using a tight pestle ("A" specification: 0.0010" - 0.0030" clearance), while keeping the homogenizer on ice. The number of strokes needed depends on the cell type used (see "Notes"). It is therefore necessary to check the homogenized cells under a phase contrast microscope after every 10 strokes. Stop when >90% of the cells are burst, leaving intact nuclei, with various amounts of cytoplasmic material attached. In most cases, the presence of this cytoplasmic contamination does not affect the final purity of the isolated nucleoli (Figure 2).

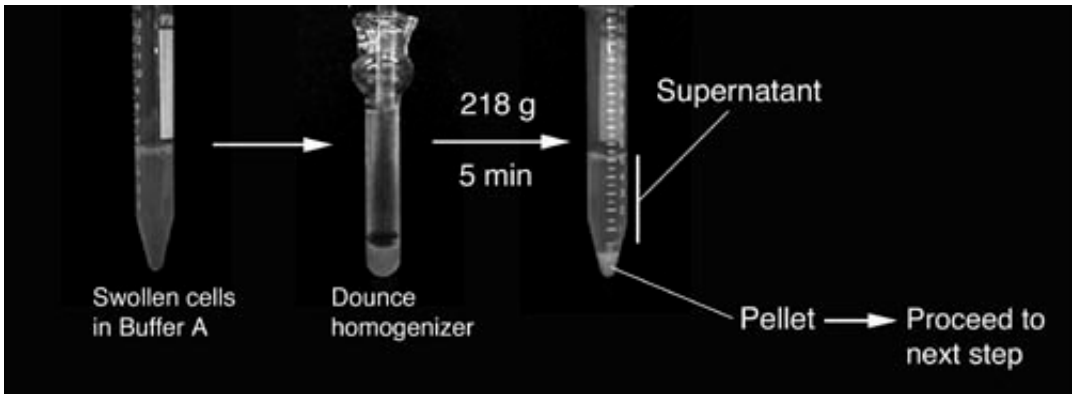

6. Centrifuge the homogenized cells at 218g (1000 rpm, Beckman GS-6 centrifuge, GH-3.8 rotor) for 5 min at 4°C. The pellet contains enriched, but not highly pure, nuclei.

7. Resuspend the pellet with 3 ml S1 solution (Figure 3). The pellet should be resuspended readily by pipetting up and down. A pellet that cannot be resuspended contains lysed nuclei and should be discarded. Layer the resuspended pellet over 3 ml of S2 solution. Take care to keep the two layers cleanly separated. Centrifuge at 1430g (2500 rpm, Beckman GS-6 centrifuge, GH-3.8 rotor) for 5 min at 4°C. This step results in a cleaner nuclear pellet (Figure 3). Resuspend the pellet with 3 ml of S2 solution by pipetting up and down.

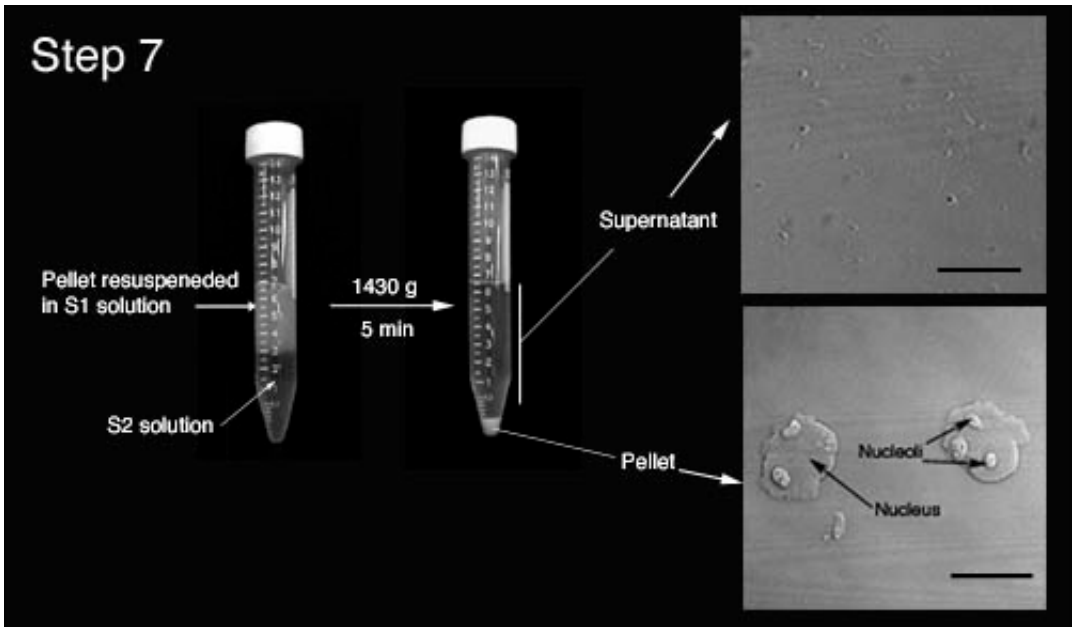

Figure 3. Step 7 of the procedure. Note the clear boundary between S1 and S2 layers before centrifugation. Insets show the DIC images of the supernatant and pellet. Note the prominent nucleoli inside the nuclei in the pellet. Bars: 10µm.

8. Sonicate the nuclear suspension for 6 x 10 second bursts (with 10 second intervals between each burst) using a Misonix XL 2020 sonicator fitted with a microtip probe and set at power setting 5 (Figure 4 Left). Check the sonicated nuclei under a phase contrast microscope. There should be virtually no intact cells and the nucleoli should be readily observed as dense, refractile bodies (Figure 4 right). The optimal sonication time depends on the cell type used. If you attempt to isolate nucleoli from a cell type from the first time, it is necessary to check the sonicated material under a microscope after every 10 seconds of sonication. Over-sonication leads to destruction of nucleoli.

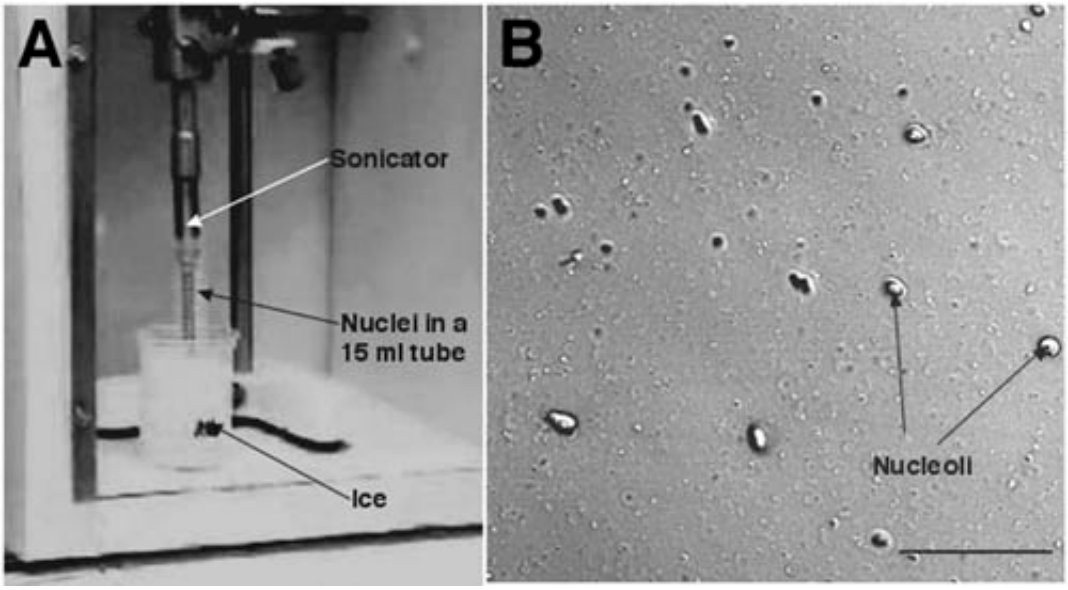

Figure 4. Left. Setup for sonication. Right. DIC image of sonicated nuclei. Note the presence of prominent nucleoli. Bar: 10µm.

9. Layer the sonicated sample over 3 ml of S3 solution and centrifuge at 3000g (3500 rpm, Beckman GS-6 centrifuge, GH-3.8 rotor) for 10 min at 4°C (Figure 5). The pellet contains the nucleoli, whilst the supernatant can be retained as the "nucleoplasmic fraction" (Figure 5).

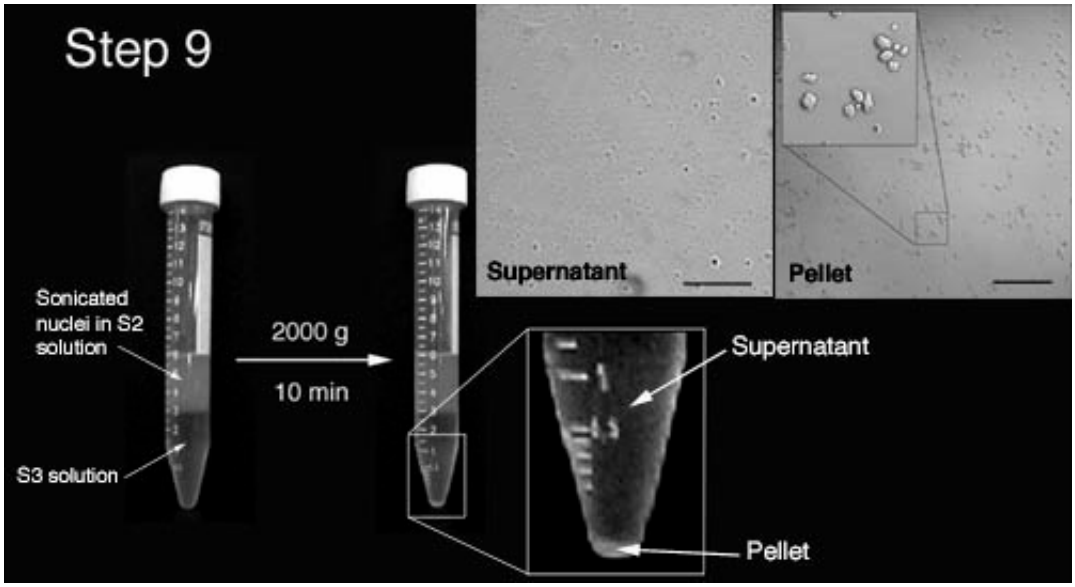

Figure 5: Step 9 of the procedure. Note the clear boundary between S2 and S3 layers before and after centrifugation. The pellet should be small but visible. Insets show DIC images of the supernatant and pellet. The pellet should contain purified nucleoli. Bars: Left inset: 10µm, right inset: 20µm.

10. Resuspend the nucleoli with 0.5 ml of S2 solution, followed by centrifugation at 1430 (2500 rpm, Beckman GS-6 centrifuge, GH-3.8 rotor) for 5 min at 4°C. The pellet contains highly purified nucleoli. Check under a phase contrast microscope to ensure this preparation contains only highly purified nucleoli without any other material (Fig 5). The nucleoli can be resuspended in 0.5ml of S2 solution and stored at –80oC.

Notes

(1) Making 2.55M sucrose stock

Here is a protocol for preparing a sucrose stock solution (Cline and Ryel,l 1971) suitable for the nucleolar isolation protocol. The resulting solution is 2.55M, or 66% by weight. Its density is 1.3224g/cm3 at 20oC, and refractive index is1.4558. The stock solution is stable indefinitely at 4oC. This procedure can be carried out at RT. There is no need to heat up the solution to help dissolving the sucrose. Heating up an incompletely dissolved sucrose solution can lead to charring of sucrose and affect the quality of the sucrose solution.

1. Weigh out 1710 g sucrose (BDH). Keep it aside in a clean container.
2. Put exactly 900ml water and a magnetic bar in a 5 litre beaker. Put the beaker on a stirrer and start stirring.
3. Add 1/3 of the sucrose into the beaker. Make sure the magnetic bar is rotating freely. Stir for 1 hour.
4. Add another 1/3 of the sucrose into the solution. Again make sure the rotation of the stir bar is not impaired. Stir for another 1 hour.
5. Add the remaining sucrose. Stir for another 1 hour, or until all the sucrose has gone into solution. The final volume should be exactly 2 litres.

(2) Sonication

We use a Misonix 2020 sonicator fitted with a microtip at power setting 5. To ensure reproducible soncation these points should be followed:

- It is necessary to tune the sonicator every time after you change the probe. Follow the manufacturer's manual for the tuning procedure.
- Sonication produces intense and localized heat in your solution. If you are concerned about the heating, the correct way to reduce heating is to shorten the sonication time and to increase the intermission between bursts. Keeping the tube on ice or performing the sonication in the cold room is helpful, but is not the most effective way of heat control.
- If the probe is too close to the liquid surface, it produces a foam and reduces the efficiency of sonication. Make sure the probe is well submerged in the solution, about 5mm above the bottom of the tube. Do not, however, touch the bottom or the wall of the tube with the probe.
- Sonicator probe that has been used repeatedly develops pits on its end. The sonication efficiency gradually decreases as time goes on. Therefore, the sonication time reecommended here can only be used as guideline. Always monitor the outcome of sonication using a phase contrast microscope. You may need to adjust the sonication time to maintain the efficiency especially if the probe is getting old. Change the probe when the efficiency is noticeably down.

(3) Analysis of the isolated nucleoli

- To immunolabel the purified nucleoli, spot about 5 µl of the nucleolar suspension on to a polylysine-coated slide (BDH Cat no: 406/0178/00), and air dry the spot. Rehydrate the slide in PBS for 5 min before carrying out a standard immunostaining procedure.
- To separate nucleolar proteins on a gel, either resuspend directly in Laemmli SDS sample buffer or in your preferred buffer. The high concentration of nucleic acid in the isolated nucleoli makes the lysed sample very viscous. The sample can be clarified by passing through a QIAshredder spin column (Qiagen Cat no: 79654). Nucleoli can also be extracted with RIPA buffer (150 mM NaCl,1% NP40, 0.5% deoxycholate, 0.1% SDS, 50 mM Tris pH 8.0, COMPLETE protease inhibitor cocktail). Immunoprecipitations can be performed from nucleolar lysates prepared in RIPA buffer.

(4) Adapting nucleolar isolation protocol to use with other cell types

The above protocol can readily be adapted to other cell types. Apart from HeLa cells, we have used this protocol, with minor modifications, to isolated nucleoli from MCF-7 (human breast epithelium), WI-38 (human fibroblast), IMR-32 (human neuroblastoma), HL60 (human promyelocytic leukemia) and plant Arabidopsis thalina cells. When adapting the protocol to a different cell type, make sure you control each step by carefully checking the products after each step under a phase contrast microscope. For example, different cell types may require a different homogenization (step 4) and/or sonication strength (step 7). The concentration of MgCl2 also appears crucial to the purity of the isolated nucleoli. If the isolated nucleoli are not pure enough, try lowering the concentration of MgCl2 in the S2 and S3 solutions. If the yield is poor, or if the nucleoli look fragmented, use more MgCl2.